Access DB# 774

SEARCH REQUEST FORM

Scientific and Technical Information Center

Requester's Full Name: Vonne Horton Examiner #: 72425 Date: 7/25/02
Art Unit: 3635 Phone Number 30 Serial Number: 09/548,876
Mail Box and Bldg/Room Location: 6D04 Results Format Preferred (circle): PAPER DISK E-MAIL

If more than one search is submitted, please prioritize searches in order of need.

****

Please provide a detailed statement of the search topic, and describe as specifically as possible the subject matter to be searched. Include the elected species or structures, keywords, synonyms, acronyms, and registry numbers, and combine with the concept or utility of the invention. Define any terms that may have a special meaning. Give examples or relevant citations, authors, etc, if known. Please attach a copy of the cover sheet, pertinent claims, and abstract.

Title of Invention: heat shielded dock pad

Inventors (please provide full names): Jason Miller et al.

Earliest Priority Filing Date: 4/13/00

***For Sequence Searches Only* Please include all pertinent information (parent, child, divisional, or issued patent numbers) along with the appropriate serial number.**

the thermal conductivity of polyurethane

and

the thermal conductivity of polyester

****

STAFF USE ONLY	Type of Search	Vendors and cost where applicable
Searcher:	NA Sequence (#)	STN
Searcher Phone #:	AA Sequence (#)	Dialog
Searcher Location:	Structure (#)	Questel/Orbit
Date Searcher Picked Up:	Bibliographic	Dr.Link
Date Completed:	Litigation	Lexis/Nexis
Searcher Prep & Review Time:	Fulltext	Sequence Systems
Clerical Prep Time:	Patent Family	WWW/Internet

	Type	Hits	Search Text
1	BRS	41011	thermal adj conductivity
2	BRS	98517	polyurethane
3	BRS	152140	polyester
4	BRS	2956	(thermal adj conductivity) and polyurethane
5	BRS	3682	(thermal adj conductivity) and polyester
6	BRS	1283	((thermal adj conductivity) and polyurethane) and ((thermal adj conductivity) and polyester)
7	BRS	1283	(thermal adj conductivity) and polyurethane and polyester
8	BRS	128025	nylon
9	BRS	2320	(thermal adj conductivity) and nylon

TRANSMISSION OF HEAT

Conduction, Convection and Radiation

Thermal Conductivity

Thermal conductivity is the measurement of the speed at which heat travels through a material through *conduction*. In the United States thermal conductivity (also referred to as the "k" value) is commonly expressed in terms of the number of BTUs of heat which will travel through one sq. foot of material which is one inch thick when there is one degree F temperature difference across the material (ie. Delta T). This expression is often stated as btu/in/hr/sq.ft/°F. The lower the "k" value the better the thermal insulation. The term "R" value is frequently used to describe the performance of insulation materials. The "R" value is simply the reciprocal of the "k" value. Therefore, the higher the "R" value, the better the insulation quality.

For example: Polyurethane foam insulation board is commonly rated at a thermal conductivity of .17 (point one seven). This means that a 1" piece of foam 12" square would permit .17 BTUs of heat to move through it in one hour if there were a temperature difference of 1^0 F on either side. Were the temperature difference across the material to be increased to 10 degrees, then the 1.7 BTUs would move through it in the same hour.

Listed below is the thermal conductivity of some common materials.

MATERIAL	CONDUCTIVITY ("k")	INSULATIVE ("R")
Copper	2712.00	.00037
Aluminum (6061)	1160.00	.00086
Aluminum (5052)	960.00	.00104
Lead	245.00	.004
Stainless Steel (316)	113.00	.00885
Glass	5.00	.20
Polyester FRP (hand laid)	.48	2.08
Polyethylene Foam	.43	2.33
Wood (dry)	.33	3.03
Polyester FRP (pultruded)	.31	3.26
Glass Wool	.29	3.45
Polystyrene (expanded)	.28	3.57
Cork Board	27	3.70
Polystyrene (extruded)	.21	4.80
PVC (Klegecell)	.21	4.80
Polyurethane Foam	.17	5.88
Air	.16	6.25
BARRIER 20 (new)	.037	27.02
BARRIER 20 (20 years)	.05	20.00
AURA Panels	.013	75.00
Total Vacuum	.004	250.00

The chart above provides generally accepted thermal conductivities typical of the materials described. Do to the variations in individual manufacturers formulations and production methods significant variations can exist between apparently similar products. It should also be remembered that thermal conductivity of the material is only one of several factors effecting the heat transfer which takes place in everyday objects. Depending on the materials involved, others factors may include *convection* (in gases and liquids) and/or *radiation* with varying emphasis on the related components *emissivity* and *absorptivity*.

Convection

In some cases the contributions of convection and radiation play only a minor part in comparison to that of conduction. However, under some conditions, the effects of one or both can be very significant. Convection is the term used to describe the motion or, circulation current, which is set up in any gas or liquid as it is heated or cooled. Convection is not, in itself, a singular heat transport vehicle as is conduction and radiation. Instead, it greatly increases conduction by constantly circulating colder material to the warm surfaces, thus increasing the effective

delta T.

A closer look at the role of "trapped air" in traditional insulation materials provides a good example of how convection effects heat transfer. As you can see from the table above, air, by itself, is a very good insulator with a "k" value of only .16. Further examination of the table shows that nearly all traditional insulation materials have a higher thermal conductivity. Therefore, one might reasonably ask, "Why use insulation at all?". The answer is found when one also considers the effect of heat transfer through convection.

The "k" value given for air (.16) describes the amount of heat which will travel directly through perfectly still, and dry, air. However, air used as an insulator never stays completely still. Instead it sets up an active circulation as one side of the containment chamber is heated. The heated air rises and the cold air falls. This circulation constantly exposes the colder air to the warm wall, thus increasing the delta T across that wall and greatly increases the rate of heat transfer through the chamber. This is where traditional insulation helps. In these materials the air is "trapped" on a great many small chambers called "cells". While each cell still sets up its own convection current, heat transfer is reduced in direct proportion to the size of the cell. The smaller the cell, the greater the reduction in convection.
In standard insulation foam, the size of the air-trapping cells is described in terms of the foam "density". A high-density foam will have a greater number of smaller cells than will a low-density foam. However, before jumping to the conclusion that the highest density foam is, inevitably, the best insulator, there is one more factor to consider. This is the thermal conductivity of the cell walls themselves. These are typically PVC, polyurethane, polyethylene or polystyrene and often have a greater thermal conductivity than does still air. The greater the number of cell walls, the more material there is present to transmit heat through conduction. This is why the best insulation foams must reach a compromise between small cell size (ie. high-density) and minimal cell wall material (low-density).

Radiation

Like conduction, radiation is a unique and independent form of heat transfer. Ignoring the conflicts of wave and quantum theory, it will suffice to say that radiation, in this case, refers to the transmission of electromagnetic energy through space. While the term radiation applies to the entire electromagnetic spectrum, our concern is with that portion which falls between visible light and radar, the infrared rays. Infrared rays are not themselves "hot", but are simply a particular frequency of pure electromagnetic energy. Sensible "heat" does not occur until these rays strike an object, thereby increasing the motion of it's surface molecules. The heat then generated is spread to the interior of the object through conduction. Therefore, radiation is fundamentally different from conduction in that it describes the transfer of heat between two substances which are not in contact with each other. All matter above absolute zero (-456.7°F) radiate heat to some degree. How much heat an object radiates is determined by it's temperature, the temperature of the surrounding environment and the object's *emissivity factor*.

Recently there has been a great deal of emphasis placed on the importance of radiant heat "barriers" by some insulation manufacturers. Such barriers inevitably consist of a piece of aluminum foil glued to a traditional air-trap type insulation foam or similar material. Although these manufacturers claim greatly increased insulation performance as a result, the truth is that the improvement, if any, is highly dependent on the application.

A radiant heat barrier works by reflecting radiant heat back toward the source. It does not reflect conducted heat, nor can it reflect heat within a solid object. In a vacuum, such as outer space, radiant heat barriers are very effective. In this air-free environment there can be no conduction (except through solid objects) so all heat transmission is by means of radiation. A radiant heat barrier on the outside of a space ship or satellite proves a very efficient insulator by reflecting back up to 95% of the radiant heat which strikes it. For this same reason, thermos bottles (ie. Dewars flasks) are also coated internally with aluminum radiant heat barriers.

However, once our space ship returns to the atmosphere of earth, it's radiant heat barrier becomes considerably less efficient. This is because the source of the heat is no longer completely radiant in nature. The warm air is also transferring heat to the ship's skin through conduction. How much good the radiant heat barrier is now doing depend on several factors. If the ship is parked on the runway in the bright sun, the percentage of radiant heat to conductive heat would be very high and the barrier would still be quite helpful. Once the ship is moved into a hot hanger, the conductive heat of the surrounding air become much more dominate and the barrier contributes little.

One example of the misuse of radiant heat barriers can be seen in the common practice of laminating foil sheets

between pieces of standard foam insulation. In this case, all heat reaching the foil barrier is conductive and passes straight through making the barrier useless. Radiant barriers reflect infrared most effectively back into a vacuum. As the density of the material in contact with the barrier increases the effectiveness decreases. A barrier which would be highly efficient in space would be totally ineffective if sandwiched between insulating foam.

The chart below gives the infrared radiation reflectivity (emissivity) of some common materials:

Material		Reflectivity
Aluminum	Bright	90-95%
	Anodized	45%
	Oxidized	70-80%
Brass	Bright	97%
	Oxidized	39%
Chromium	Polished	92%
Copper	Bright	95%
	Oxidized	22%
Steel	Polished	45%
	Oxidized	15%
Nickel	Polished	95%
	Oxidized	5%
Zinc	Bright	77%
	Oxidized	77%
Paint	White	10%
	Black	14%
Rubber		6%
Water		8%

For further information on insulation see our Technical Library and main Insulation Page.

Plastics

Microstructure and Engineering Applications

Second edition

N J Mills

School of Metallurgy and Materials,
University of Birmingham

ARNOLD

A member of the Hodder Headline Group
LONDON

Metallurgy and Materials Science

a series of student texts

First published in Great Britain 1986
Second edition 1993

British Library Cataloguing in Publication Data

Mills, Nigel
Plastics: Microstructure and Engineering
Applications. – 2Rev. ed. – (Metallurgy
& Materials Science Series)
I. Title II. Series
668.4

ISBN 0-340-56043-6

2 3 4 5 6 7 8 9 10

Typeset in 10/11½ Times by Wearset, Boldon, Tyne and Wear.
Printed and bound at Replika Press Pvt. Ltd., 100% EOU,
Delhi 110 040, India

10

Transport properties

When substances travel through polymers the intention may be to restrict the transport to a minimum level, as with water transport through a LDPE damp-proof membrane, or to maximise the transport, as with the use of pipelines. There will be intermediate cases where selective transport is required—separating gases, or separating salt from water in a desalination plant. The subject of the design and use of pipes is covered in Chapter 13, so the main topic here is film products that transport limited amounts of substances. Solid transfer through polymer sheet is impossible, but woven polymers or polymer grids allow solid transfer on different scales. The optical properties of films are important in their commercial applications, and the transmission of light via fibre optics is explored because of its revolution of telecommunication links. The transmission of heat through solid polymers uses many of the same concepts as gaseous diffusion, so it is convenient to treat it here. The transmission of electrons and electromagnetic radiation is dealt with separately in Chapter 11 because of the size of the topic.

10.1 GASES

10.1.1 Solubility

The transport rate of gases through a polymer film depends both on the solubility of the gas in the polymer and on its diffusion coefficient. The solubility of the gas is affected by the strength of the intermolecular forces between pairs of gas molecules. In Chapter 1 the nature of the van der Waals bond was described. The strength of the bond can be characterised by the depth E_0 of the potential energy well shown in Fig. 1.1. Table 10.1 gives values of this constant for some common gases. E_0 measures the propensity of a gas to condense inside a polymer.

For the gases down to oxygen in Table 10.1 it is usually found that the gas concentration C is related to the gas pressure p by Henry's law

$$C = Sp \tag{10.1}$$

where the constant S is the solubility constant for the gas. Gas concentration

Table 10.1 van der Waals bond energies and solubilities in the amorphous phase in polyethylene

Gas	E_0 (10^{-23} J)	S^* (10^{-6} mol m^{-3} Pa^{-1})
He	14	5.4
H_2	52	—
N_2	131	18.4
O_2	163	34.3
CH_4	204	90.6
CO_2	261	201

can be expressed in various units; in S.I. units it is in mol m^{-3}, but it is more common to use m^3 of gas at STP per m^3 of polymer. Conversion between the units is made using the molar volume (at 0 °C, 1 bar) of 22.4×10^{-3} m^3. Solubility is expressed in S.I. units as mol m^{-3} Pa^{-1} (where 1 Pa = 1 N m^{-2} = 10^{-5} bar); a reduction to the base units of kg, m, s is not made because it confuses calculations.

In semi-crystalline polymers such as polyethylene and polypropylene that are above their glass transition temperatures the solubility constant is found to be proportional to the volume fraction V_{am} of the amorphous phase

$$S = V_{am}S^* \tag{10.2}$$

The solubility constant for 100% amorphous material S^* increases with the van der Waals bond energy.

For the more soluble gases such as methane and carbon dioxide the solubility behaviour is more complex, particularly for glassy polymers, for which the difference between the volume expansion coefficients of the liquid and glassy states is large. The values of $\alpha_L - \alpha_G$ for PET, PC and PMMA are 8.0, 4.3 and 1.3×10^{-4} C^{-1} respectively, and only the first two of these glassy polymers show this anomalous effect. Some of the gas is physically adsorbed on the surface of submicroscopic holes in the polymer. Fig. 10.1 shows how the concentration of CO_2 increases with pressure p in PET, a polymer that is used in carbonated drinks containers. The solubility equation is modified to

$$C = Sp + \frac{abp}{1 + bp} \tag{10.3}$$

The second term on the right is the *Langmuir adsorption isotherm* which describes the equilibrium concentration of gas molecules on a surface. The gas molecules bombard the surface and some of them stick; this process is in equilibrium with the rate of desorption from the surface. The area of the internal holes per unit volume of polymer is the disposable constant a, known as the hole saturation constant [7.9 cm^3 (STP)/cm^3] and b is the ratio of the adsorption to desorption rates (0.35 bar^{-1}) for CO_2 in PET. This Langmuir term dominates the solubility at pressures below 5 bar. The gas that is adsorbed on internal surfaces plays little part in gas transport through the polymer, and it can be ignored in calculations of gas permeation.

Water vapour is a gas with an anomalous solubility characteristic, this time because of the strong hydrogen bonding between the molecules. Fig. 10.2

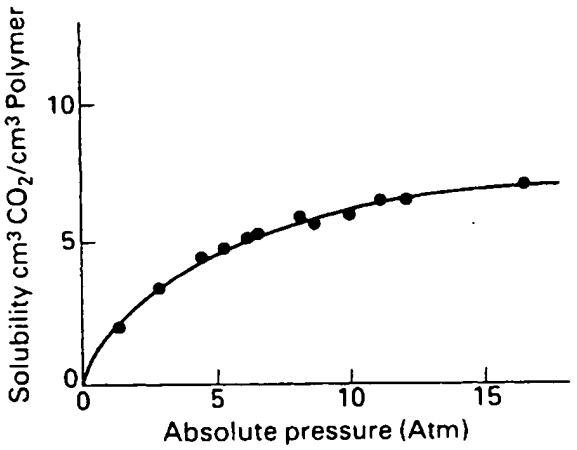

Fig. 10.1 Solubility of CO_2 at 25 °C in polyethylene terephthalate versus the gas pressure (from Hopfenberg (ed.), *Permeability of Plastic Films and Coatings*, Plenum Press, 1974)

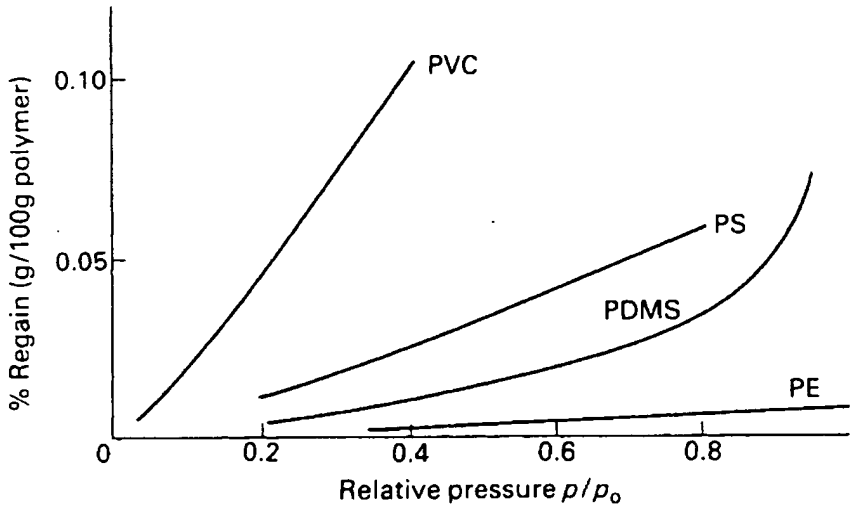

Fig. 10.2 Solubility of water vapour in various polymers versus the relative pressure (= vapour pressure/saturation vapour pressure) at 25 °C (PDMS at 35 °C) (from Crank and Park (eds.), *Diffusion of Polymers*, Academic Press, 1968)

shows that the sorption isotherms can curve steeply upwards as the relative pressure approaches 1. However, hydrophobic polymers such as polyolefins still obey Henry's law.

10.1.2 Steady state diffusion

The mathematics of diffusion of a gas in a polymer is exactly the same as for the diffusion of heat considered in Chapter 4. Thus, although the permeation constant is defined by steady state conditions, there may be significant transient effects. In considering the steady state transfer of a gas at a pressure p_1 on one side of a polymer film of thickness L, to a pressure p_2 on the other side (Fig. 10.3) there are two ways of defining the transfer constant. The gas concentration will be constant at C_1 and C_2 respectively in the polymer at the

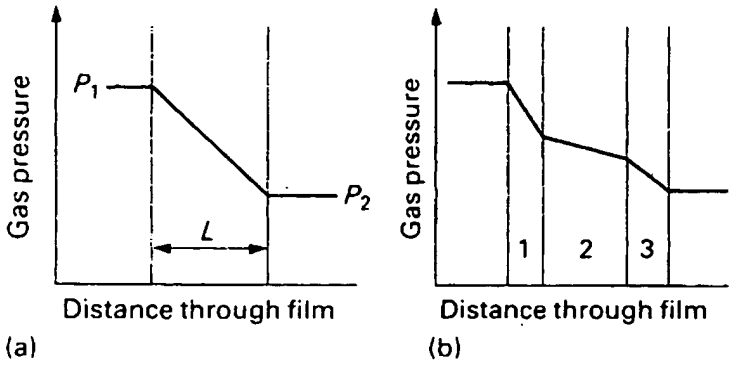

Fig. 10.3 Variation of gas pressure through a single polymer film, and a multilayer film in which the polymers 1, 2 and 3 have different permeabilities, when there is a steady state gas flow

two surfaces. The flow rate through an area A of film is then given either by

$$Q = DA\left(\frac{C_1 - C_2}{L}\right) \tag{10.4}$$

or

$$Q = PA\left(\frac{p_1 - p_2}{L}\right) \tag{10.5}$$

where D is the *diffusivity* and P the *permeability*. There are many different units in which these constants are quoted, because the apparatus used to determine them may measure gas volumes or mass changes, and the pressure units and time units can vary. The diffusion constant has the simple units $m^2\ s^{-1}$ so long as both Q and C use the same units for the amounts of gas. Table 10.2 gives some values for pure polymers in the unoriented state.

The diffusivity is related to the permeability by

$$P = DS \tag{10.6}$$

so the S.I. units of permeability are mol m^{-1} Pa^{-1} s^{-1}. As 1 mol of gas at standard temperature and pressure (STP) occupies 22.4 litres, it is also possible to use the units m^3 (STP) m^{-3} bar^{-1} s^{-1}. American permeability data are usually quoted in Imperial units using 'mil' (0.001 inch) for thickness, and a standard test area of 100 in^2. Older European data can be in cgs units, with pressure measured in cmHg. Hence the following conversion factors for permeability may be useful.

$$\frac{\text{mol}}{\text{m Pa s}} = 4.91 \times 10^{17} \frac{\text{cc mil}}{100\ \text{in}^2\ \text{atm day}}$$

$$= 2.95 \times 10^{5} \frac{\text{cm}^3\ \text{(STP)}}{\text{cm cmHg s}}$$

$$= 2.95 \times 10^{15}\ \text{barrer}$$

where

$$1\ \text{barrer} = 10^{-10}\ \text{cm}^3\ \text{(STP)}\ \text{cm}^{-2}\ \text{cmHg}^{-1}\ \text{s}^{-1}$$

Table 10.2 Permeability data and diffusion constants at 25 °C

Polymer	Permeability (mol m^{-1} Pa^{-1} s^{-1}) O_2 $\times 10^{-18}$	H_2O $\times 10^{-15}$	CO_2 $\times 10^{-18}$	Diffusion constant (m^2 s^{-1}) O_2 $\times 10^{-12}$	CO_2 $\times 10^{-12}$
Dry EVAL (33%E)	0.02				
PVDC	1.3	0.7	7		0.001
PET	14	60	30	0.36	0.054
PVC rigid	23	40	98		
Nylon 6	30	135	200		
Polyether sulphone	340		1900		2.0
HDPE	400	4	1000	17	12
LDPE	1100	30	5700	46	37
PP	400	17	1000		
PC	500	470	2900		5.3
PS	580	330	4000	12	1.3
Polyphenylene oxide	780		3000		
Butyl rubber	370		1500	80	5.8
Natural rubber	7000	770	37 000	158	110
Silicone rubber	205 000	14 500	1 095 000	1700	

For semi-crystalline polymers above T_g with a variable crystallinity the permeability is no longer proportional to the volume fraction amorphous phase V_{am}. This is because the gas must diffuse through the channels between the lamellar crystals, and the detailed morphology depends on the polymerisation, catalyst type, the thermal history and whether there is any orientation in the film. The permeability is found to be proportional to V_{am}^{n} where the exponent n lies between 1.2 and 2 for different polymerisation routes. The effect on the permeability of the molecular weight M of the gas is approximately described by $P \propto M^{-0.5}$. This is not followed rigorously and it can be seen from Table 10.2 that the permeability of CO_2 in glassy polymers is higher in proportion to the oxygen permeability than it is for semi-crystalline polymers.

10.1.3 Transient effects in gaseous diffusion

There are transient effects when a plastic container is filled with gas. Fick's second law, derived in Appendix A, applies so long as the diffusion coefficient is independent of the gas concentration C. The differential equation for the gas concentration C, for one-dimensional diffusion along the x axis, is

$$\frac{dC}{dt} = D\frac{d^2C}{dx^2} \tag{10.7}$$

where t is time and D is the diffusion coefficient. The variation of D with temperature is described by

$$D = D_0 \exp\left(-\frac{E_D}{RT}\right) \tag{10.8}$$

where E_D, the activation energy for diffusion, is a measure of the rate at which D increases with increasing temperature, R is the gas constant and T the absolute temperature. The diffusion coefficients will be highest in semi-crystalline polymers if the amorphous phase is above its glass transition temperature T_g. Table 10.2 gives diffusion data for polyethylenes at 25 °C. The reason for the higher diffusion coefficient in LDPE is that the crystalline phase has a negligible diffusion coefficient, and LDPE has a higher percentage amorphous content. Equation (A.17) shows that after a time t the oxygen concentration will exceed 50% of its surface level in a layer x thick where

$$x = 0.94\sqrt{Dt} \tag{10.9}$$

When Fick's second law is obeyed the analytical methods in Appendix A can be used to predict the total flow of the gas through the film. If the film is initially free from the diffusing gas, and a constant concentration C is applied at time $t = 0$ at one surface, the total amount V that passes through unit area of sheet thickness L is given by

$$\frac{V}{LC} = \frac{Dt}{L^2} - \frac{1}{6} - \frac{2}{\pi^2}\sum_{n=1}^{\infty}\frac{(-1)^n}{n^2}\exp\left(-\frac{Dn^2\pi^2 t}{L^2}\right) \tag{10.10}$$

Fig. 10.4 shows the amount that diffuses through the sheet as a function of the elapsed time. The graph settles down to a steady permeation rate, and if this straight line is extrapolated back it cuts the time axis at a *time lag* t_L given by

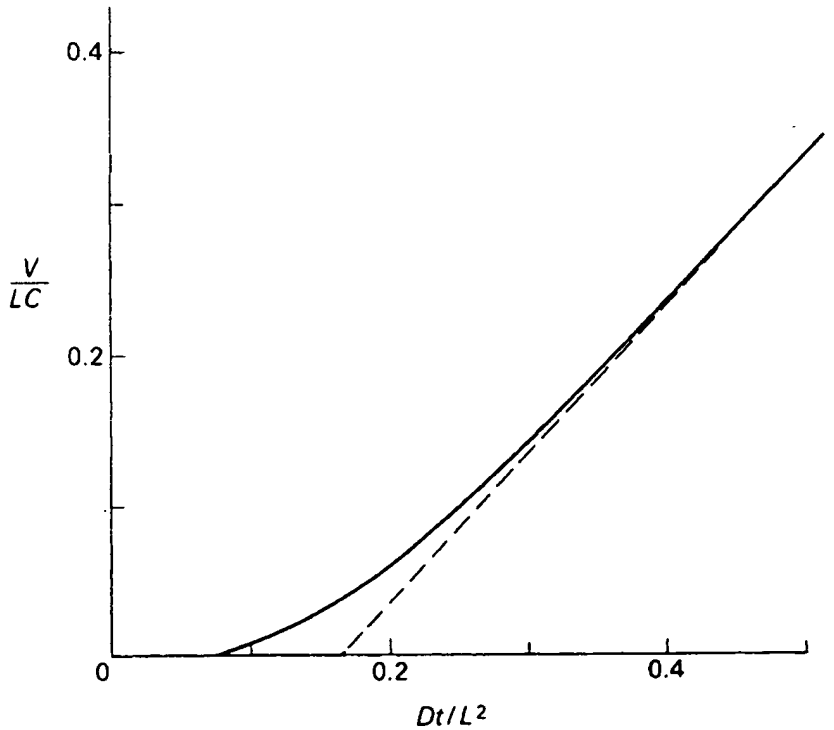

Fig. 10.4 Volume of gas passing through 1 m² of sheet of thickness L versus time according to equation (10.10)

$$t_L = \frac{L^2}{6D} \tag{10.11}$$

For natural gas (methane) passing through a 3 mm thick MDPE pipe wall, the time lag is 10.4 days, as $D = 1.0 \times 10^{-11}\ m^2\ s^{-1}$. Consequently a steady state permeation test with this pipe is a long term experiment. If the diffusion constant is independent of concentration and Henry's law holds, then the diffusion constant can be calculated from the permeability.

Where the diffusion coefficient D increases with the gas concentration, equation (10.7) is replaced by

$$\frac{\partial C}{\partial t} = \frac{\partial}{\partial x}\left(D\frac{\partial C}{\partial x}\right) \tag{10.12}$$

This equation is best solved by finite difference methods on a computer. This case occurs with organic vapours diffusing through rubbers, and can occur with high concentrations of gases in glassy polymers (Fig. 10.1) where the gas swells the glass and can alter the T_g value.

10.1.4 Packaging applications

Biaxial orientation is often used to improve the in-plane tensile strength and toughness of polymer films. This also decreases the permeability, the main reason being the increase in crystallinity on stretching—see Fig. 7.18 for PET. It is useful to have data for the barrier properties of particular thickness films, to allow materials selection and package design. For multilayer films made by coextrusion or coating techniques the total permeability P_{TOT} is related to the total thickness L by

$$\frac{P_{TOT}}{L} = \frac{P_1}{L_1} + \frac{P_2}{L_2} + \ldots \tag{10.13}$$

It is often more convenient to be able to add directly the *resistance to the gas transfer* for each layer, defined as

$$R_i \equiv \frac{L_i}{P_i} \tag{10.14}$$

where L_i is the layer thickness, and then to calculate the steady state gas flow from

$$Q = (p_1 - p_2)/(R_1 + R_2 + R_3 + \ldots) \tag{10.15}$$

Table 10.3 gives some film resistances for commercially important films. Low density polyethylene, because of its domination of the film market, acts as a reference material by which others can be compared. Its good water vapour resistance cannot be improved upon by a large factor, but its oxygen resistance is relatively poor. Even the oxygen resistance of PET in the biaxially oriented form is not good enough for the preservation of oxygen sensitive foodstuffs such as beer. Consequently PET bottles can have an outer coating of a PVDC copolymer to meet this requirement. The oxygen

resistance of each 4 μm thick PVDC coating can be calculated from the data in Table 10.3 as 3150 GN s mol^{-1}. The PVDC coating is sprayed on to the outside of completed bottles, and it is not capable of being recycled. The initial pressure loss in a carbonated drink bottle when it is filled is a result of transient diffusion and the Langmuir adsorption of the CO_2 in the PET.

Table 10.3 Strength and gas resistance data

Polymer	Film thickness (μm)	Tensile strength (kN m^{-1})	Oxygen resistance (GN s mol^{-1})	Water vapour resistance (GN s mol^{-1})
LDPE	25	0.35	23	0.8
Chill cast PP	32	0.9	45	1.4
Biaxially oriented PP	14	3.5	45	1.2
Biaxially oriented PET	12	2.0	1700	0.32
Biaxially oriented PET + 4 μm coat of PVDC	20	2.5	8000	2.5

Extruded ethylene vinyl alcohol copolymer (EVAL) is used as an oxygen-barrier packaging material. When EVAL is dry it has an extremely low permeability to oxygen, but the vinyl alcohol part of the copolymer is highly hydrophilic, and in the swollen wet state the permeability increases (Fig. 10.5) to be higher than that of PVDC. The construction of a multilayer squeezable bottle, for foods such as ketchup that are sensitive to oxygen yet

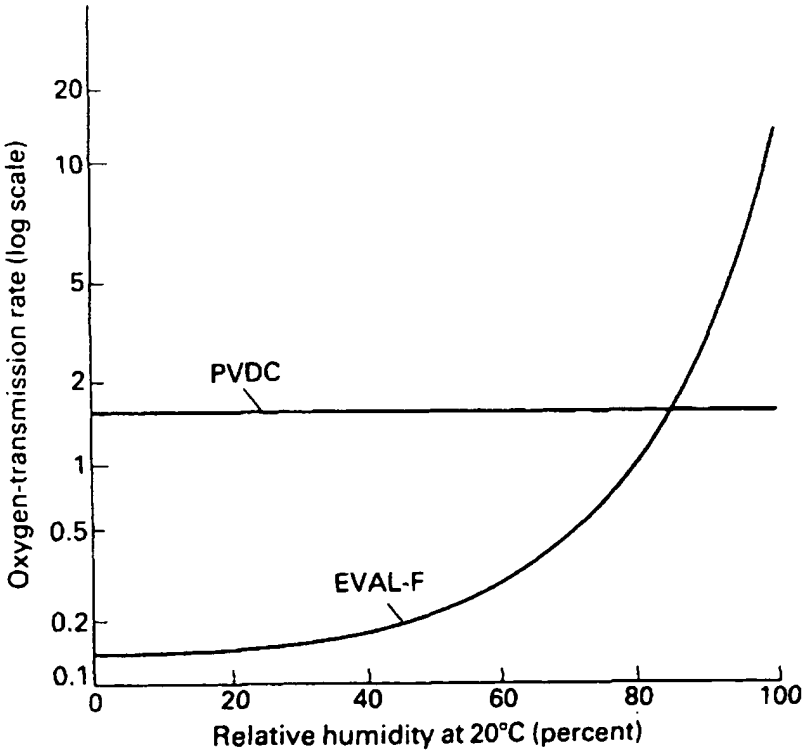

Fig. 10.5 Variation of the oxygen transmission rate (cm^3 m^2 day^{-1} bar^{-1} for 20 mm film) with relative humidity for the high barrier PVDC and EVAL films (from *Plastics Engineering*, 1984, May, 43, Soc. Plastics Eng. Inc.)

need to be sterilised in the container when it is filled, presents a difficult problem. Biaxially stretched PET is insufficiently form stable at 100 °C because the T_g of the amorphous phase is only 80 °C. Polypropylene has an adequate form stability but far too high an oxygen permeability. If a layer of EVAL is sandwiched between inner and outer layers of polypropylene then the oxygen resistance can be achieved so long as the EVAL remains below a 75% R.H. level. The problem is the sterilisation step, because the permeability of all polymers rises rapidly as the temperature increases (Fig. 10.6). Consequently the EVAL layer is at nearly 100% R.H. after sterilisation. If the EVAL layer is placed near the outside of the polypropylene sandwich then the water resistance of the outer polypropylene layer is lowered and the EVAL humidity can drop to an acceptable level within a week or so of filling the container. There are five layers in the container since there is a 0.6 μm thick layer of adhesive between the polypropylene and EVAL. The design of co-extrusion dies to produce a stable melt parison with five distinct layers is a formidable problem.

For a single material film, the rate at which water vapour permeates

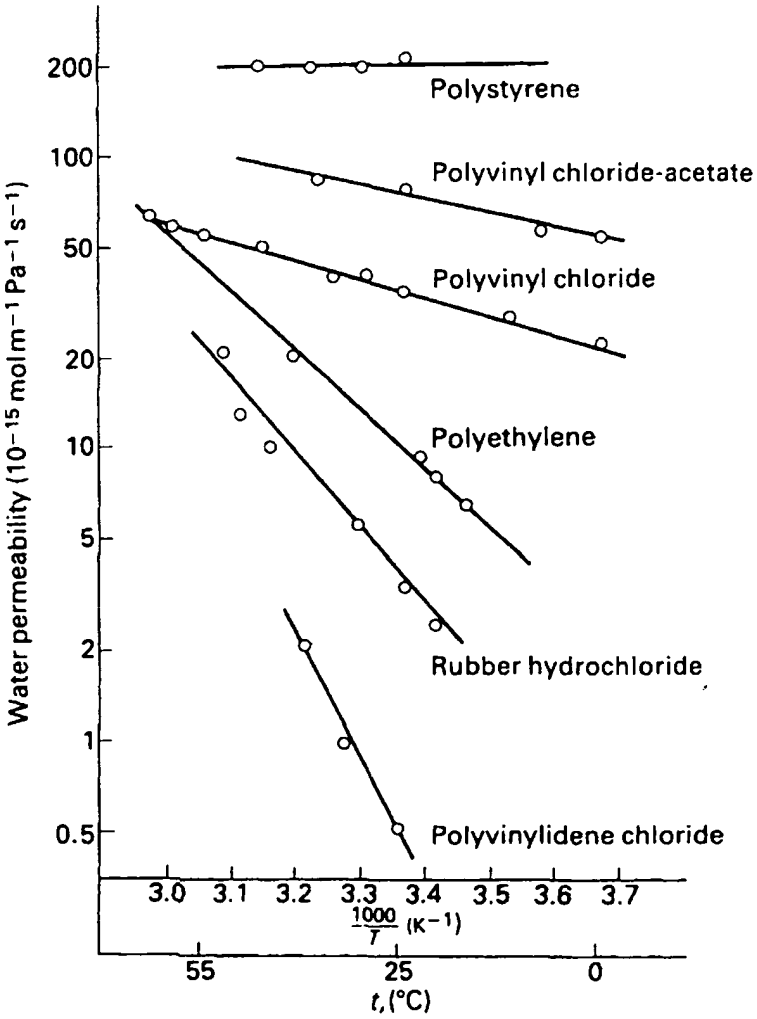

Fig. 10.6 Variation of water permeability with reciprocal absolute temperature (from Hennessy *et al.*, *The Permeability of Plastics Films*, Plastics and Rubber Inst., 1966)

through increases with temperature more rapidly than the permeability data in Fig. 10.6. This is because the vapour pressure of water in mmHg increases rapidly with temperature (17.5 at 20 °C, 55.3 at 40 °C, at 60 °C, 355.1 at 80 °C). From the definition

$$\text{relative humidity} \equiv \frac{\text{partial pressure of water vapour}}{\text{vapour pressure of water at that temperature}} \qquad (10.16)$$

it follows that the water transport rate through the film is proportional to the permeability, to the water vapour pressure and to the relative humidity difference across the film.

10.1.5 Gas separation

With developments in the efficiency of gas separation membranes they have become competitive with other methods of gas separation. In Chapter 1 the separation of gaseous products of cracking naphtha was carried out by liquefaction and fractional distillation of the liquids at high pressure and low temperature. If gaseous separation can be carried out at ambient temperatures there are great savings in energy and the plant is more compact. The developments necessary have been in achieving high permeation rates while having mechanical durability. Equation (10.4) shows that to achieve high gas transport rates, the film thickness must be very small, the area of film must be large, and both the permeability and the applied pressure must be large. The contradictory requirements of having a thin film that can cope with a high pressure of up to 100 bar, have been met either by using porous fibres with a thin membrane skin, or by having porous layers that are cloth reinforced, with a thin skin of a polymer. Figure 10.7 shows the construction of a porous polysulphone fibre that has been spun from a water miscible solvent into water.

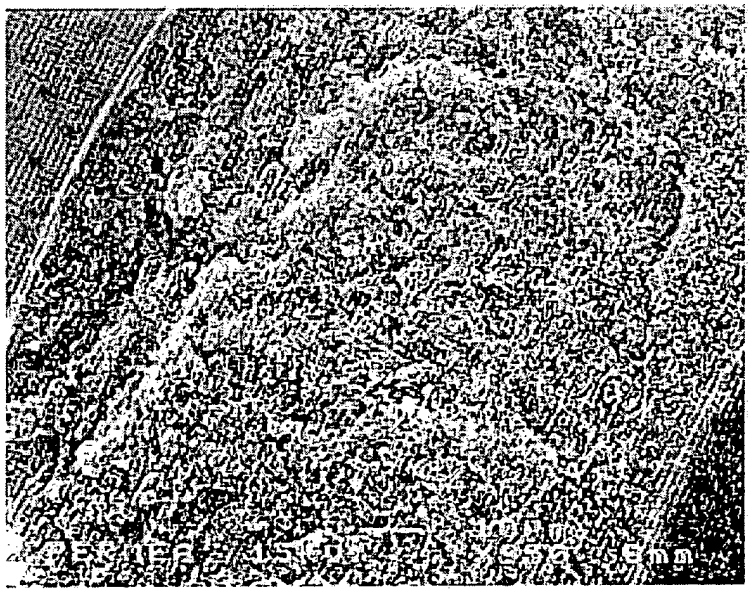

Fig. 10.7 Scanning electron micrograph showing close up of the wall of a prism-α hollow membrane used in gas separation applications. (Reproduced with kind permission of Permea Inc., St. Louis, USA.)

One area of application is in the provision of 99% pure nitrogen supplies from air, in competition with deliveries of liquid nitrogen or bottles of high pressure nitrogen. The selectivity α of a polymer membrane is defined as

$$\alpha \equiv \frac{P_A}{P_B} \tag{10.17}$$

where A and B are the two gases. When A is oxygen and B is nitrogen the values for most polymers lie in the range 3 to 5. Although this is inadequate to produce the required purity in a single separation stage, chemical engineers are used to multi-stage processes, and a second separation of the nitrogen rich output of the first stage will produce the required purity. Table 10.2 suggests that silicone rubber would be a good membrane material, but it is mechanically weak. Hence the need for a strong but porous support. The development of porous polysulphone layers or fibres has provided such a support.

One advantage of membrane separation systems is that they can be used for a variety of operations in the chemical industry. The permeability of gases increases as the size of the molecule decreases, so it is possible to separate small amounts of hydrogen from a mixture of gases. Applications are reviewed by Spillman (1989).

10.2 LIQUIDS

The diffusion of liquids into polymers is in general slower than the diffusion of gases. The diffusion coefficients are of the order of $10^{-13}\,m^2\,s^{-1}$. The major difference is that the equilibrium solubility can be much larger than that of gases, and the liquid content can change the diffusion constant, or even the physical state of the polymer. Semi-crystalline polymers are in general more resistant to organic liquids than are glassy polymers, so these will be dealt with separately.

Many hollow containers for liquids are made by the blow moulding of polyolefins, especially HDPE. They are used to contain a great variety of liquids because direct attack by environmental stress cracking or dissolution is relatively rare. High molecular weight grades with good ESC resistance can be blow moulded, and to improve the resistance still further MDPE copolymers can be used (see Chapter 8). There is, however, an affinity between polyethylene and aromatic or chlorinated hydrocarbons; they swell the amorphous phase of the polyethylene and have relatively high permeabilities. Table 10.4 lists the permeabilities of several common liquids. The corresponding figures for LDPE are a factor of ten larger, showing that diffusion through the amorphous rubbery phase dominates the permeability. Ethyl acetate is a representative constituent of foodstuffs. The high permeability of alkanes is not surprising considering the chemical similarity with polyethylene.

One application for blow moulded polyethylene containers is as petrol tanks for cars. There are considerable weight savings, corrosion is eliminated and the complex moulded shapes can fit into spaces above the rear axle.

Table 10.4 Permeability of liquids through HDPE of density 950 kg m^{-3} at 23 °C

Liquid	Permeability (g mm m^{-2} day^{-1} bar^{-1})
Toluene	37.5
n-Heptane	17.1
97 octane petrol	16
Ethyl acetate	1.6
Diesel oil	0.5 to 3
Methanol	0.15

Volkswagen used about 100 000 per year in the Passat model. Large containers have an advantage in terms of permeation because the surface area to volume ratio decreases as the volume increases (this also applies to carbonated drinks bottles, which is why the 2 litre PET bottles were introduced first). The container is designed to withstand a certain internal pressure; 3 bar for petrol tanks in spite of crash tests showing that internal pressures did not exceed 1 bar. Blow moulding does not produce a uniform wall thickness product; values ranging from 4 to 7 mm are found for a petrol tank. Consequently it might appear that the loss of petrol by permeation through HDPE tank walls would be insignificant. However the EEC regulations set a limit of 10 g emission over 24 hours at 23 °C, and US regulations the tighter limit of 2 g per 24 hour shed (sealed house emission determination) test, because hydrocarbon gas emissions can lead to photochemical smog. The constituents of petrol swell polyolefins, and the diffusion rate after 1 year is not acceptable, so some extra treatment is necessary. At present the polyethylene is sulphonated (treated with concentrated SO_3) to decrease the permeability of a surface layer by a factor of 10 (Fig. 10.8), or fluorinated to

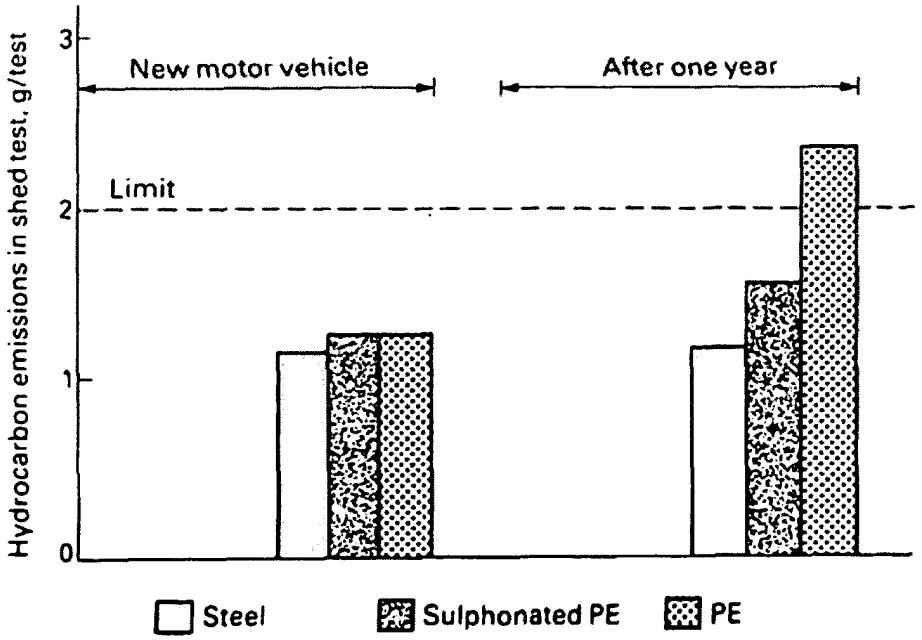

Fig. 10.8 Hydrocarbon emissions from steel, polyethylene, and sulphonated polyethylene fuel tanks (from *Automotive Engineering*, 1982, **90**, 68, Society of Automotive Engineers Inc.)

decrease the permeability by 97%. An alternative in future would be to use multilayer blow mouldings, or platelets of a less permeable polymer within the HDPE.

When polymers are used as food containers the additional problem of extraction of additives from the polymer arises. This is because certain food constituents diffuse into the polymer. For example fats or soils in many foods can diffuse readily into polyethylene. If the fat has a strong affinity for a polymer stabiliser or antioxidant the equilibrium concentration in the fat will be much higher than that in the polymer. There will be a two way diffusion process with the food component entering the polymer and the polymer additive entering the foodstuff. Fig. 10.9 shows some experimental results for a fat tricapryllin in contact with HDPE containing 0.25% of the hindered phenol antioxidant BHT. The results for different diffusion times at 40 °C are normalised by using $x/\sqrt{t}$ as the horizontal axis. The concentrations of both diffusants remain low and the results fit the theory for a constant diffusion coefficient of 5×10^{-13} m^2 s^{-1} for the fat and 1×10^{-14} m^2 s^{-1} for the antioxidant. There are two consequences of the extraction phenomenon. Firstly only certain non-toxic additives are permitted in polymers that are to be used as food containers. Secondly if a plastic container is re-used with another foodstuff then constituents of the first foodstuff may diffuse back out of the polymer into the second foodstuff. This is noticeable if polyethylene beakers or bottles are filled with orange squash, then re-used with water.

A third application area exists when the flow of a liquid through a polymer film is to be *maximised*. This arises in water treatment where seawater or brackish water can be purified by reverse osmosis, and in biomedical applications such as blood dialysis units for kidney patients. The design problem is to find a polymer of a high permeability for water, yet low

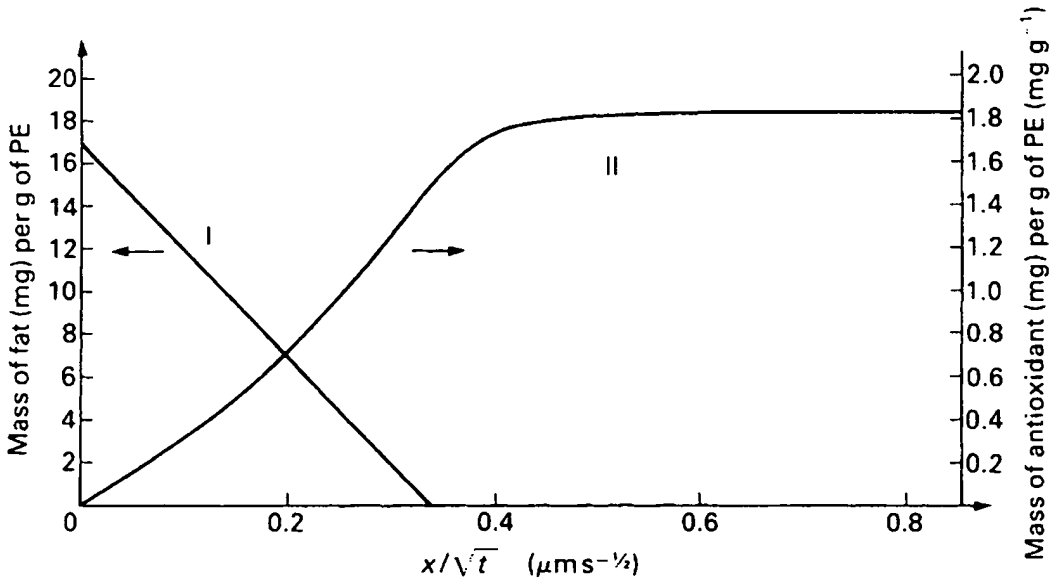

Fig. 10.9 Diffusion of a fat into HDPE and of an antioxidant additive from the HDPE, plotted against x/t where x is the distance from the surface and t the time (from *Angewa. Macromol. Chem.*, 1979, **78**, 179, Hüthig and Wepf Verlag)

permeability for the salt. To maximise efficiency the membrane area must be large and its thickness as small as possible consistent with a lack of pinholes. It is an advantage to apply a high pressure to one side of a reverse osmosis membrane. Because the membrane is thin, it is mechanically unable to resist the pressure unless it is supported on a backing structure. Fig. 10.10 shows the construction of a cellulose triacetate membrane on a porous cellulose nitrate–cellulose acetate support. To make the unit compact the composite membrane is spirally wound on to an inner cylinder, and the edges glued together. When a pressure of 70 bar is applied to the seawater side, NaCl rejection levels in excess of 99.7% can be achieved.

There are clothing applications where it is required to allow the passage of water vapour and to prevent the passage of water. The ingenious solution

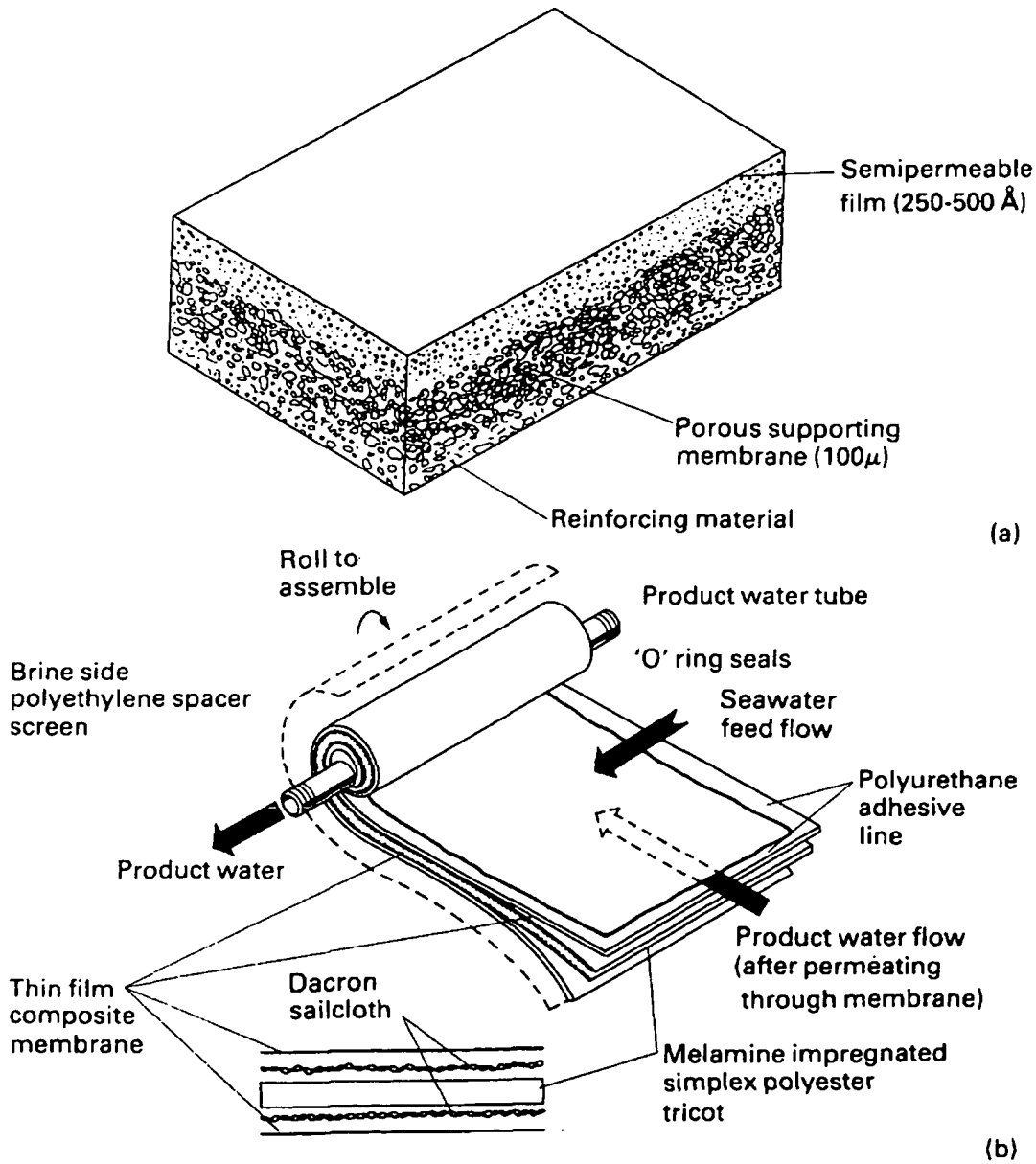

Fig. 10.10 (a) Cross section of a composite membrane for reverse osmosis of sea water. (b) Spiral winding of the membrane to make a compact unit (from Hopfenberg (ed.), *Permeability of Plastic Films and Coatings*, Plenum Press, 1974)

utilised in the Goretex fabrics is to stretch PTFE film in a manner that produces microscopic voids (Fig. 10.11). These allow the passage of water vapour from the skin but the very low surface energy of PTFE means that liquid water cannot wet the surface of the film and hence rain cannot be drawn through it by capillary action.

10.3 SOLIDS

In order to give some idea of how polymeric meshes or fabric can be used to prevent the passage of solids, some of the civil engineering applications of 'geotextiles' will be explored. The two main product types are both based on highly oriented polyolefins, the requirements being low cost and high strength. One type utilises polypropylene film that has been uniaxially drawn and fibrillated to produce a low cost substitute for fibres. This is woven into a coarse textile with a mass of between 100 and 300 g m^{-2} and a thickness of 0.3 to 0.7 mm (Fig. 10.12). The more recently developed Netlon products are based on the uniaxial or biaxial drawing of perforated HDPE sheets. These have a hole size that is an order of magnitude larger (up to 100 mm).

As well as having barrier properties, these geotextiles are very strong in tension in the plane of the product, so can be used for soil reinforcement. Soils have zero tensile strength, and steep sided soil embankments can fail by shear on surfaces at 45° to the vertical, especially if they contain clay and become waterlogged. Horizontal layers of geotextile, with a tensile strength of 50 to 100 kN per m width, can be incorporated into embankments at 1 m vertical separation, while the embankment is constructed. The plane of the geotextile is that in which the tensile principal stress of the soil acts, so it is efficient in its reinforcement action. Because the geotextile is buried it cannot be degraded by UV radiation.

Fig. 10.13 shows another application of the unidirectionally oriented

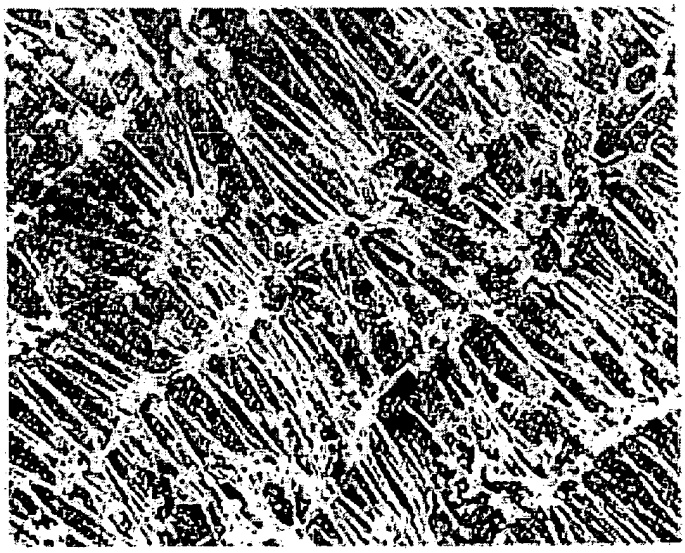

Fig. 10.11 SEM micrograph of Goretex fabric showing the pore structure that allows the passage of water vapour. (Courtesy of WL Gore & Associates (UK) Ltd.)

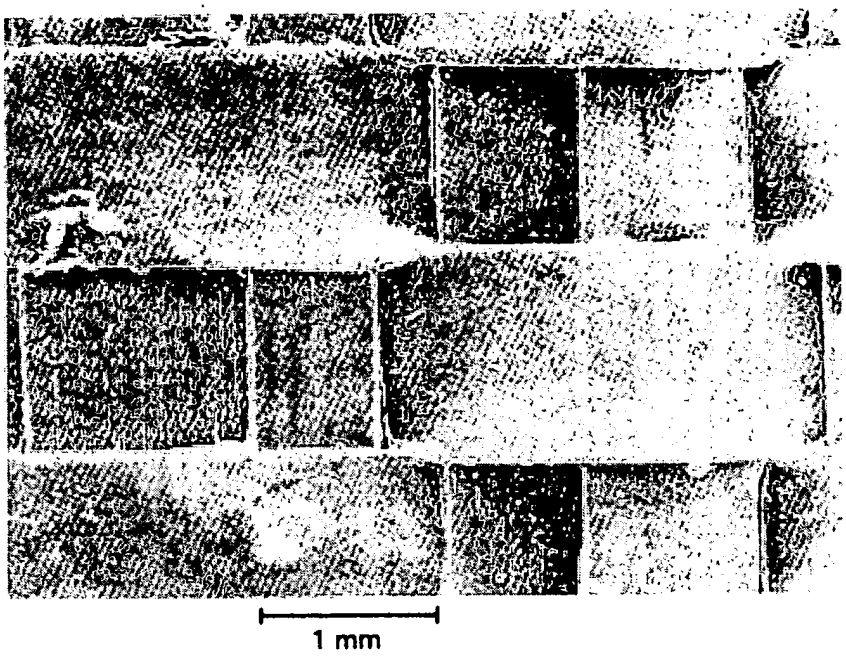

Fig. 10.12 Woven mesh of fibrillated polypropylene film used to allow water permeation but prevent the ingress of fine soil particles

Netlon product. Vertical rods couple the faces of the cellular structure, which can then be filled with granular material to form a 1 m thick stable 'mattress' at the foot of an embankment on top of soft soil.

Woven geotextiles prevent the loss of fine soil particles across the fabric plane. If the water flow is unidirectional across the textile a filter cake of fine particles builds up upstream of the textile and this aids the filtration process. By preventing road stone from being punched into soft underlying soil the total amount of road stone used can be reduced. The shear strength of the road stone layer is preserved without the ingress of fine soil particles. It also appears that geotextiles allow drainage in the plane of the fabric, so that in Fig. 10.13 water can drain to the sides of the embankment. This can aid the consolidation of a newly constructed embankment.

A third type of product that aids water drainage, but does not have the soil reinforcing element of geotextiles is the perforated corrugated pipe shown in Fig. 10.14. The hoop direction corrugations are produced by specially shaped cooling sections that move down the cooling section of an extrusion line on a caterpillar track. The corrugations provide a maximum resistance to diametral crushing by soil loads, and yet allow flexibility for coiling the pipe. Rectangular holes are punched in the small diameter regions and these allow the ingress of water into the drainage pipe. The elastic deflection δ that occurs when a line load of q N per unit length is applied to the pipe is given by

$$\delta = 0.0186 \frac{qD_m^3}{EI} \tag{10.18}$$

Since the mean diameter D_m of the pipe cannot be altered the deflection can only be limited by increasing the second moment of area I per unit length.

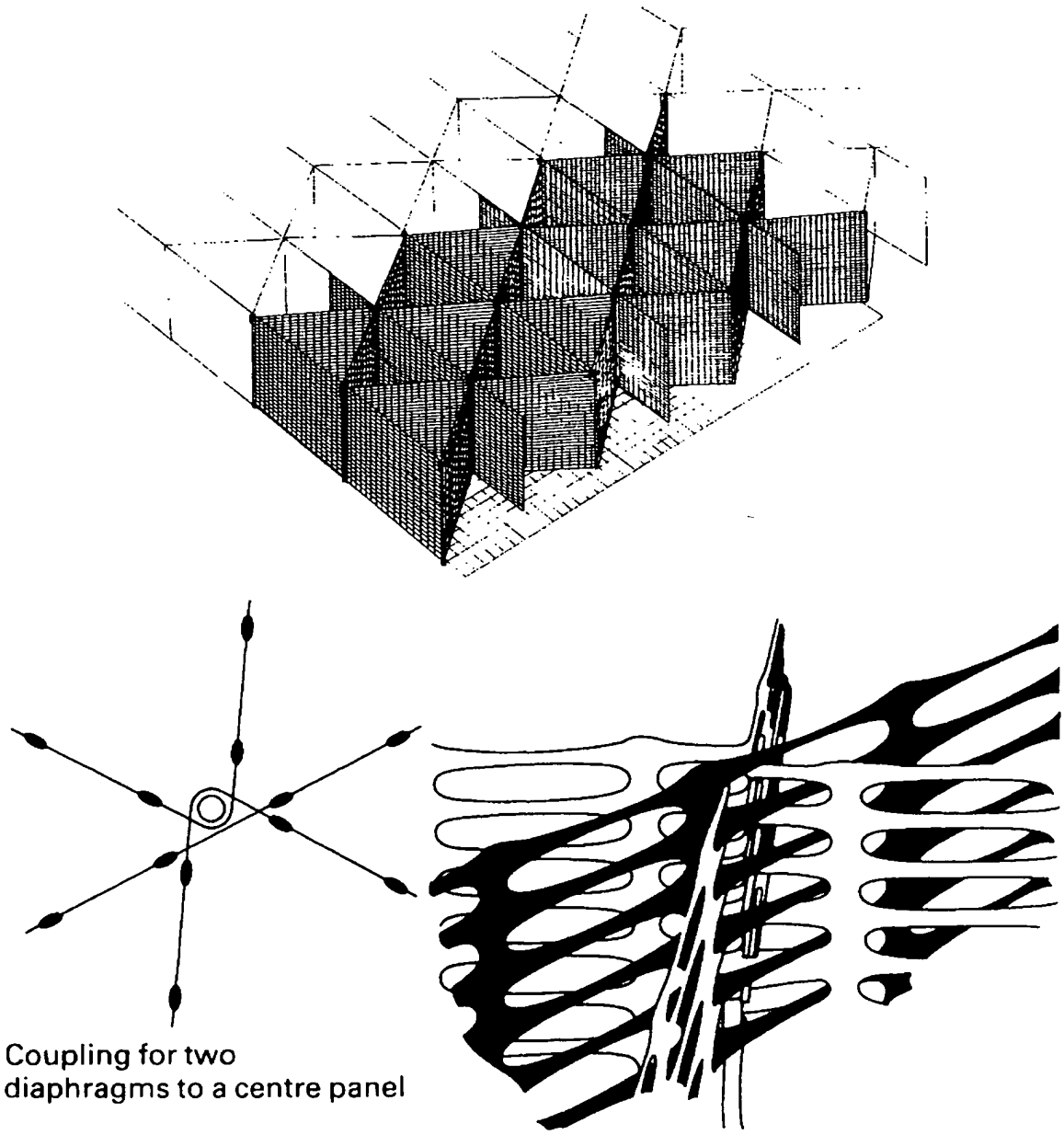

Fig. 10.13 Use of unidirectionally drawn perforated HDPE sheet to construct the vertical walls of triangular cells, that form a reinforcing mattress at the base of an embankment (from *Tensor Geocell Mattress* pamphlet, courtesy of Netlon)

This has a value

$$I = \frac{t^3}{12} \tag{10.19}$$

for a cylindrical pipe of thickness t. For the corrugated pipe the actual cross section in Fig. 10.14 can be approximated by a trapezoidal wave of wavelength L and crest length C. The I_c value of this shape is

$$\frac{I_c}{I} = 1 + \left(\frac{H}{t}\right)^2 \left(1 + \frac{4L}{C}\right) \tag{10.20}$$

if the vertical thickness remains equal to t. H is the height of the wave shape.

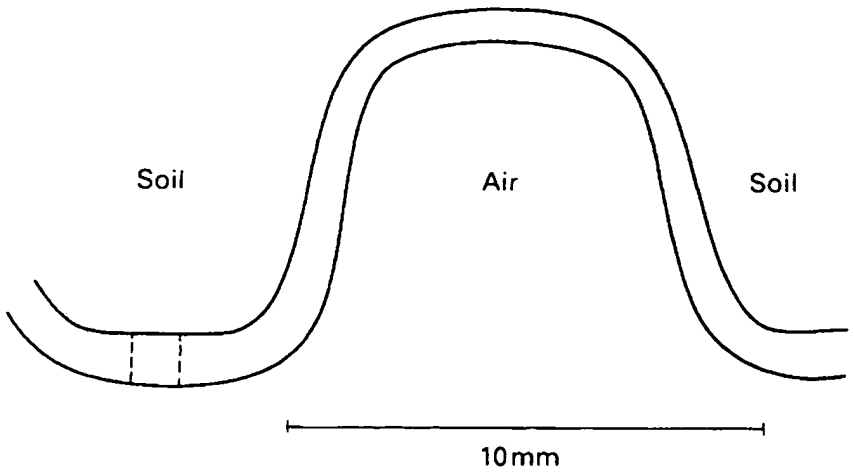

Fig. 10.14 Section through the wall of a corrugated PVC pipe, of diameter 150 mm, used for soil drainage. Slots of size 8 mm × 1 mm are punched at intervals in the base of the corrugation to allow water ingress

For the shape shown the stiffening factor calculated from equation (10.20) is approximately 450; this is equivalent to a materials savings of 87% compared with a cylindrical pipe of equal bending stiffness.

10.4 LIGHT

10.4.1 Refraction and reflection of light

The high optical clarity plastics are PMMA, PC and thermosetting diallyl glycol carbonate (tradename CR39). These glassy materials have a much lower Young's modulus (3 GN m^{-2} as against 70 GN m^{-2}) and tensile strength (50–70 MN m^{-2} as against over 200 MN m^{-2}) than conventional soda-lime glass. Usually only the infrared and ultraviolet components of the light are absorbed by the polymer, unless there are pigments present, or the polymer contains conjugated double bonds. The advantage of these polymers lies in their lower density and greater toughness, and the fact that they can be moulded to high precision, obviating the polishing stages needed with silicate glasses.

Table 10.5 Optical properties of glassy polymers

Material	Refractive index, n_Y	Dispersive power, D	Density, ρ (kg m^{-3})	$\frac{\rho}{n_Y - 1}$	Stress optical coefficient (10^{-12} m^2 N^{-1})
PMMA	1.495	0.0189	1190	2400	4
CR-39	1.498	0.0172	1320	2650	34
PC	1.596	0.0333	1200	2010	78
PS	1.590	0.0323	1060	1800	9
Soda-lime silica glass	1.520		2530	4870	2.7

If the plastic is to be used in lens applications then the refractive index value and the dispersive power D are important. The refractive index is

measured for particular yellow (587 nm), blue (486 nm) and red (656 nm) wavelengths and D calculated from

$$D = \frac{n_B - n_R}{n_Y - 1} \tag{10.21}$$

where n_B is the refractive index for blue light, n_R is the refractive index for red light and n_Y is the refractive index for yellow light. Table 10.5 shows that polycarbonate has a high refractive index, which allows lenses to be lighter, but the high dispersive power will increase chromatic aberrations.

The mass of a lens of a given diameter and focal length is proportional to the axial thickness of the lens and to the material density. If the radius of curvature of both surfaces of a biconvex lens is R then the focal length f is given by

$$f = \frac{R}{2(n-1)} \tag{10.22}$$

As the axial thickness of the lens is proportional to $1/R$, equation (10.22) shows that it will also be proportional to $1/(n-1)$. Hence the mass of the lens

$$m \propto \frac{\rho}{n-1}$$

Values of this quantity are given in Table 10.5, where it will be seen that plastic lenses allow considerable mass savings.

Fig. 10.15 shows the phenomena that occur when light meets a sheet of plastic at normal incidence. About 4% of the light intensity will be reflected back at the air/polymer and at the polymer/air interfaces; the reflected intensity R_0 for normal incidence is related to the incident intensity I by

$$R_0 = \left(\frac{n_1 - n_2}{n_1 + n_2}\right)^2 I \tag{10.23}$$

where the refractive index of the polymer $n_1 \cong 1.5$, and that of air $n_2 = 1$. If a high reflectivity is required (see the CD manufacture in Chapter 13) a conducting coating is required. Metals have a complex refractive index, with real part n_R and imaginary part n_I. This means that the light wave penetrates the metal with an exponentially decaying amplitude. The magnitude E of the electric vector varies with the distance y in the metal as

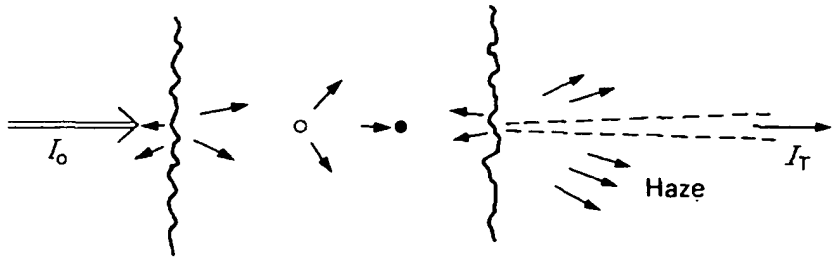

Fig. 10.15 Processes in a plastic film that reduce the transmitted light intensity

$$E = E_0 \exp(-\omega n_I y/c) \cos \omega(t - n_R y/c) \tag{10.24}$$

where ω is the frequency of the wave and c the speed of light. For solid sodium at a wavelength of 589 nm the components of the refractive index are $n_R = 0.04$ and $n_I = 2.4$. This leads to a reflectivity for thick films of $R = 0.9$. For thin films the amplitude of the transmitted light decreases, according to equation (10.24), as $\exp(-2\pi n_I y/\lambda)$. This means that the metal only needs to be a few wavelengths thick for the reflectively to be high. Such thicknesses can easily be applied by vacuum evaporation, and the main concern is the protection of the layer from abrasion, with a transparent lacquer.

10.4.2 Light scattering

Light scattering can occur at the polymer/air interface, and internally in the polymer (Fig. 10.15). Different applications can tolerate different levels of light scattering. If the transmitted light just provides illumination, as in a roof light, or allows a liquid level to be inspected, as in a brake fluid reservoir, then a high level of light scattering can be tolerated. However if the light allows the performance of an eye–limb coordination task, like driving a vehicle, then a high level of optical clarity is required. Small angle deviations of the light path, caused by the lens effects of a non-planar plastic surface, will cause image distortion. High angle light scattering will cause glare from any bright light source in the field of view such as oncoming headlights at night.

Light scattering is marked in semi-crystalline polymers with a spherulitic microstructure, so unpigmented polyethylene appears milky and opaque. Light scattering is negligible when the inclusions in the matrix are of a diameter smaller than 10% of the wavelength of the light (Fig. 10.16). There

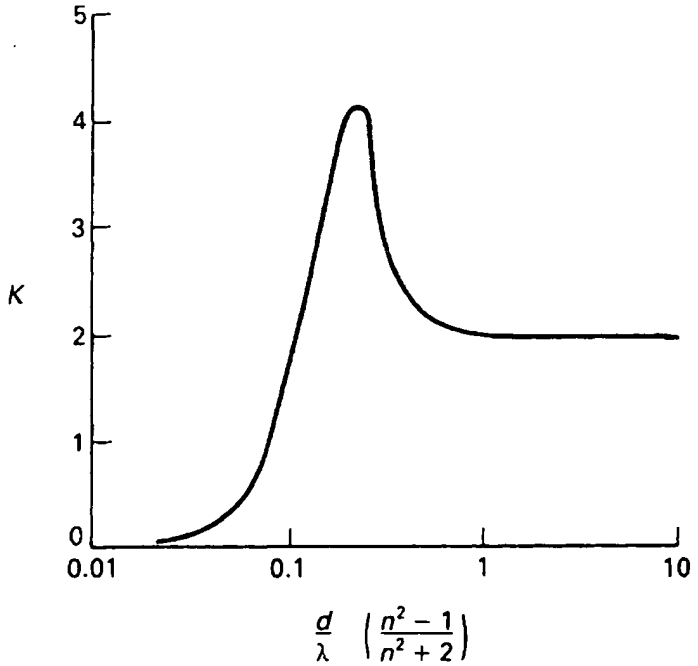

Fig. 10.16 Scattering coefficient for a single sphere of relative refractive index n versus the ratio of the sphere diameter d to the wavelength of the light λ

is a diameter at which the scattering coefficient peaks before it settles down to a constant value for large spheres. The scattering also depends on the difference $n_1^2 - n_2^2$ according to equation (10.17).

The mean refractive index n of a phase is related to the density ρ (and to the constant mean polarisability of the monomer unit α) by

$$\frac{\bar{n}^2 - 1}{\bar{n}^2 + 2} = C\rho\bar{\alpha} \tag{10.25}$$

where C is a constant. For most semi-crystalline polymers the density of the crystalline phase is greater than that of the amorphous phase (Table 10.6) and the width of the crystal lamellae is of the same order as the wavelength of visible light. The exceptional case of polymethylpentene is one where the crystal has very open helical chain conformations, and the resulting semi-crystalline polymer is transparent. Nearly all rubber toughened polymers such as ABS are opaque because the phases differ both in density and polarisability.

Table 10.6 Densities of polymer phases at 20 °C

Polymer	Crystal density ($kg\ m^{-3}$)	Amorphous density ($kg\ m^{-3}$)
Polyethylene	1000	854
Polypropylene	940	850
Polymethylpentene	820	840

Even if a semi-crystalline polymer could be made 100% crystalline, there would be light scattering from neighbouring crystals that have different orientations. The anisotropy of bonding means that polymer crystals have a different refractive index n_c for light polarised along the covalently bonded **c** direction than it does for light polarised along the crystal **a** or **b** axes. Stretching the product aligns the **c** axes of crystals, and if crystallisation occurs on heating from the glassy state the high nucleation density results in a crystal size much smaller than λ. This is why the walls of PET carbonated drinks bottles are transparent.

The optical properties of polyolefin packaging films are important. If extrusion is carried out at too high a speed a surface roughness occurs on the molten extrudate and this will increase the light scattering. The average spherulite size in polyethylene film must be kept below the wavelength of light to minimise light scattering.

The scratching of glassy plastics (Section 7.2.5) will cause light scattering. The surface can be made more abrasion resistant by coating them with a hard layer of a highly crosslinked silicone thermoset. The layers are 5 to 10 μm thick and the tensile failure strain at 1.2% is smaller than that of the substrate. Consequently the presence of a brittle surface layer reduces the toughness of the product (see Section 8.3.3). This is less of a problem for spectacle lenses than it is for motorcycle visors, which are designed to cope with 145 km h^{-1} impacts of a 7 mm ball bearing.

10.4.3 Fibre optics

Fibre optics are the equivalent of pipes for light in that there is total internal reflection at the fibre/coating interface. Fig. 10.17 shows the propagation of a ray down the fibre. The refractive index of the fibre n_f must be less than that of the coat n_c so that the angle of incidence γ at the interface is greater than the critical angle θ_c, given by applying Snell's law

$$n_f \sin \theta_c = n_c \tag{10.26}$$

The amount of light that can enter the flat end of the fibre and be transmitted along it by total internal reflection is determined by the semi-acceptance angle α, given by applying Snell's law at the end face of the fibre

$$\sin \alpha = n_f \sin \beta \tag{10.27}$$

Assuming that there is a uniformly bright plane emitter at a fixed distance from the end of the fibre, the light gathering power of the fibre P is proportional to the square of sin α_c and to the cross sectional area of the fibre. By equation (10.27) this gives

$$P \propto n_f^2 \sin^2 \beta_c$$

and since $\beta + \gamma = 90°$ use of equation (10.26) gives

$$P \propto n_f^2 - n_c^2 \tag{10.28}$$

The right hand side of equation (10.28) is defined as the square of the numerical aperture of the fibre. The materials selection problem with fibre optics is to coat the fibre with a low refractive index that is durable and which protects the fibre. It might be thought that uncoated fibres would work well, but it would then be possible for light to pass between touching fibres, and the damaged caused by contact would cause losses.

There are several types of fibre optics and the requirements on losses determines the type of material used. Table 10.7 shows that the long distance telecommunication application has very stringent requirements on the transmission losses. These can only be met if the light travels axially down the fibre as a single mode wave (similar to a waveguide for cm wavelength radar waves). Fig. 10.18 compares the losses of the high purity silica fibres that are

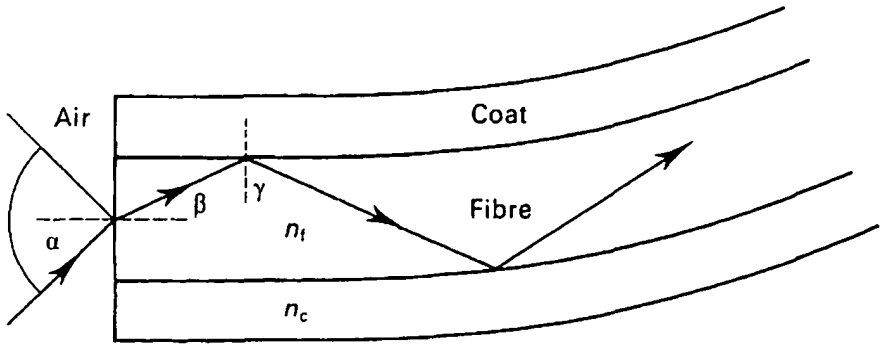

Fig. 10.17 Ray diagram for light passing down a fibre optic cable, showing the limiting ray that just undergoes total internal reflection. $n_f = 1.65$, $n_c = 1.50$, numerical aperture = 0.69, limiting $\alpha = 43°$

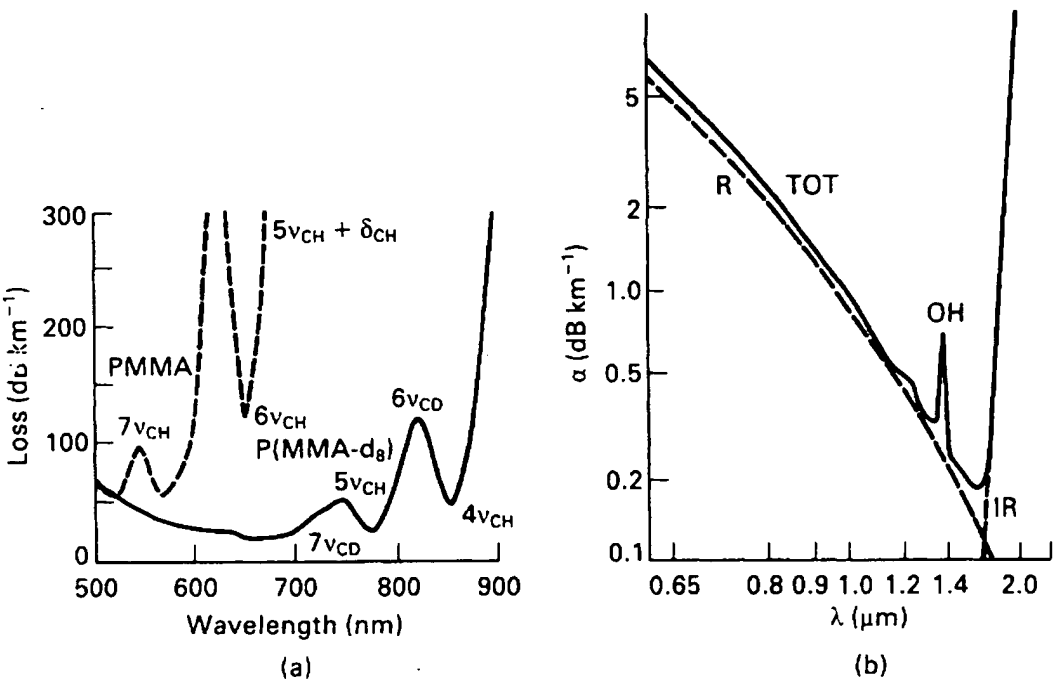

Fig. 10.18 Transmission losses versus wavelength for (a) PMMA and deuterated PMMA (from Kaino and Katayama, *Polym. Eng. Sci.*, 1989, **29**, 1209 and (b) pure silica single mode fibre. R is the Rayleigh scattering, IR the infrared absorption and OH the hydroxyl absorption (from *Philips Tech. J.*, 1989, **44**, 245)

used with that of ordinary and deuterated PMMA. The loss peaks are due to various molecular vibrations. In the PMMA these are harmonics of the C—H bond vibration, and the absorption becomes very strong in the infrared region. In the silica fibre there is a loss peak at 1.4 μm due to absorbed hydroxyl groups. There is a background effect of Rayleigh scattering, due to variations in the density of the material, which decreases as λ^{-4}. This explains why the telecommunications fibres operate with laser light at 1.30 μm or 0.85 μm, where the Rayleigh scattering is a minimum. Plastics are used as the outer protection of telecommunication fibres to prevent damage to the glass coating and to minimise bending of the fibres. A rubber interlayer is used between the outside of the 250 μm diameter glass and the 900 μm diameter UV-cured glassy polyacrylate secondary coating. The transmission losses of polymer cored fibres have been reduced by using fluorinated structures and avoiding the C—H bond. However the lower limit to the transmission loss is thought to be 5 dB km^{-1} at a wavelength of 0.65 μm.

The use of polymer fibres is preferred where flexibility is important. This could be, e.g., for supermarket bar-code readers, or endoscopes for observation in difficult-to-reach places. The medical use of endoscopes is growing since no tissue needs to be cut to reach the point of observation, and various cutting tools can be attached to the endoscope. Flexibility is achieved by having many fibres of small diameter—the theory of this is dealt with in Section 11.2.1. The PPMA fibres can be bent to much higher strains than could a silica fibre.

Table 10.7 Types of fibre optic system

Application	Type of transmission	Losses (dB km^{-1})	Core/coat diameter (μm)
Telecommunications	Single-mode wave	<0.4	8/125
Local area networks	Multi-mode waves	~0.6	50/125
Endoscopes	Ray	>500	250

10.5 THERMAL BARRIERS

The thermal conductivity of solid polymers is always within a factor of two of 0.3 $W m^{-1} K^{-1}$, with the higher values occurring in highly crystalline polymers. Thermal barrier materials have become increasingly important as the price of energy has risen, which has led to the development of low thermal conductivity building materials. If these materials can at the same time act as a barrier to water, and have some mechanical strength, so much the better. We shall consider the development of polyurethane foams and polystyrene foams for building applications.

In a closed cell foam there are a number of mechanisms that contribute to the overall thermal conductivity. The main ones are the thermal conductivity of the polymeric cell walls, the conductivity of the gas and convection and radiation in the cells. For foams of density 30 kg m^{-3} the cell wall contribution is small. Convection inside the cells makes a negligible contribution for cell diameters smaller than 10 mm, and the radiation contribution is predicted to be linearly proportional to the cell size. Fig. 10.19 shows the effect of varying the cell size of polyurethane foams; there is clearly an advantage in minimising the cell size. With polystyrene foams the cells are rarely larger than 0.1 mm so radiation is expected to play a minimal part in the conductivity of the foam. The gas contribution can be estimated by following the changes in thermal conductivity with time. The fluorocarbon gas $CFCl_3$ used with polyurethane foam has a negligibly small diffusion coefficient through polyurethane. However, this is not true for the CO_2 gas initially present, or for oxygen and nitrogen which diffuse in from the air. Air has a higher thermal conductivity (0.024 $W m^{-1} K^{-1}$) than the fluorocarbon gas (0.009 $W m^{-1} K^{-1}$). Replacements of CFC gases with pentane or CO_2 to protect the ozone layer will have to take this into account.

Fig. 10.20 shows the change in the thermal conductivity value with time; the increase is due to the ingress of air and an increase in the total pressure of gas in the cells. The gas conductivity clearly dominates the total response. Heat loss calculations for buildings must be based on the long term value. Since polyurethane foam is invariably used with facings (paper, glass fibre, plasterboard, glass fibre reinforced concrete, etc.), the overall U value of the product must be calculated (in watts per m^2 area per degree temperature differential). This can be calculated from the thicknesses L_i and conductivities k_i of each layer using

$$\frac{1}{U} = \frac{A(T_i - T_0)}{q} = h_i + \frac{k_1}{L_1} + \frac{k_2}{L_2} + \ldots + h_0 \qquad (10.29)$$

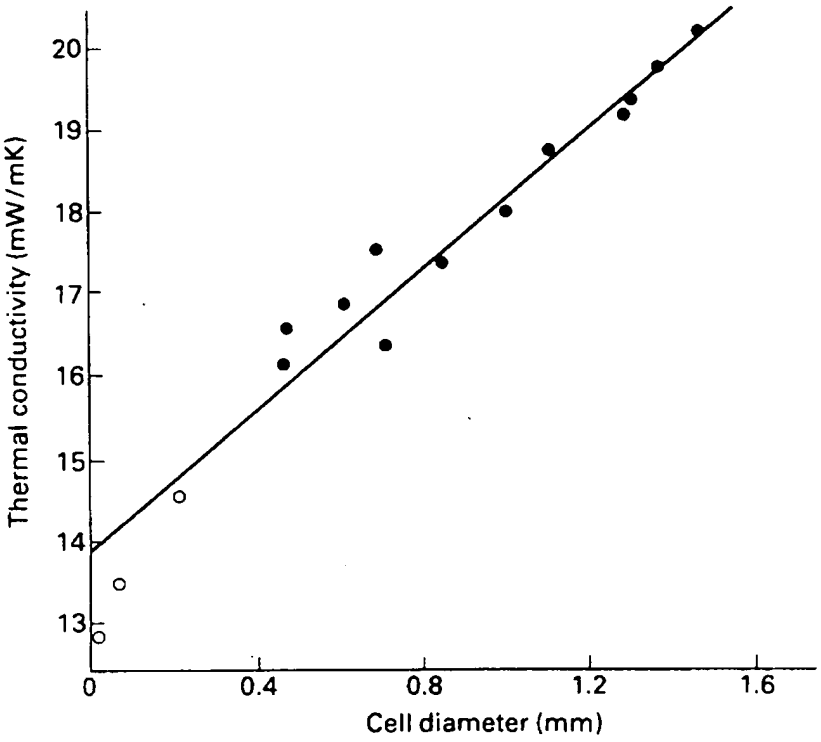

Fig. 10.19 Thermal conductivity of a polyurethane foam and of a fixed density versus the mean cell size (from J. M. Buist (ed.), *Developments in Polyurethanes*, Elsevier Applied Science, 1978)

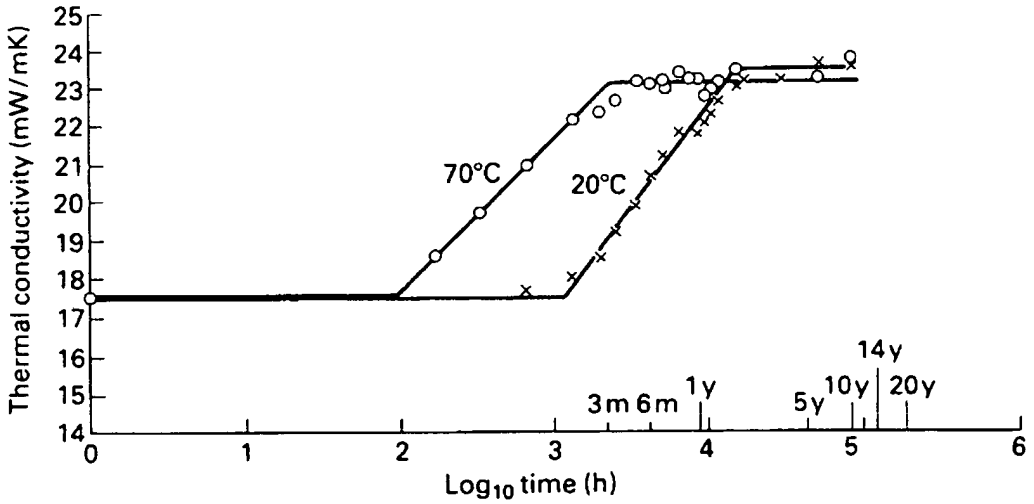

Fig. 10.20 Variation of the thermal conductivity of polyurethane foam with storage time (from J. M. Buist (ed.), *Developments in Polyurethanes*, Elsevier Applied Science, 1978)

The heat transfer coefficients h_0 at the outside is probably high enough when there is forced convection to contribute nothing to the overall U value. Current UK building regulations call for a maximum U value of $0.6\,W\,m^{-2}\,K^{-1}$ for walls. This can be achieved using a 25 mm layer of polyurethane foam of density 30 to 35 $kg\,m^{-3}$. At this level of insulation the losses from windows become significant—a single glazed wooden frame

window has $U \cong 5\ W\ m^{-2}\ K^{-1}$, whereas a double glazed PVC framed window has $U \cong 2.5\ W\ m^{-2}\ K^{-1}$.

Polyurethane foam forms a good adhesive bond to most surface layers, and it has a relatively high Young's modulus. Consequently the sandwich structure performs efficiently in terms of bending stiffness per unit panel mass (Chapter 3). This has allowed the development of lightweight panels for use in roofs and walls. If thermal insulation is of paramount importance, as in cold stores, the foam thickness can be increased to 125 mm.

Polystyrene foam has somewhat different applications because of its physical form (expanded beads) and different properties (a much higher permeability to water and less effective adhesion to facing materials). The expansion gases pentane and steam escape fairly rapidly from the foam, so the thermal conductivity of the foam filled with air is about twice that of the best polyurethane foam—a 50 mm thick slab of foam has a U value of 0.5 to $0.6\ W\ m^{-2}\ K^{-1}$. The bead-like form of the foam allows it to be mixed directly with concrete to form a low density ($850\ kg\ m^{-3}$) and low thermal conductivity ($0.13\ W\ m^{-1}\ K^{-1}$) concrete. The compressive design strength of $4\ MN\ m^{-2}$ is still adequate because the mortar matrix takes the majority of the load so this expanded polystyrene concrete can be used to make thermally insulating blocks and walls. Loose polystyrene beads have been used to fill the cavities between the inner and outer leaves of house walls. If they are loose they are liable to settle or escape, so the beads are bonded together with adhesive. The water barrier properties of the bonded bead filling are inferior to the original air gap, with a 45% increase in water transfer.

Table 4.4.4 Thermal Conductivities for Building Insulation

Material	Bulk density, lb/ft³	Temp, °F	k
Balsam wool, blanket	3.6	70.	0.021
Cabot's Quilt, eelgrass	15.6	86.	0.027
Glass wool, blanket	3.25	100.	0.022
Hairfelt, blanket	11.0	86.	0.022
Insulating boards, Insulite, Celotex, etc.	12–19	100.	0.027–0.031
Kapok, DryZero, blanket	1.6	75.	0.019
Redwood bark, loose, shredded, Palco Bark	4.0	100.	0.025
Rock wool, loose	7.	117.	0.024
Sil-O-Cel powder	10.6	86.	0.026
Vermiculite, loose, Zonolite	8.2	60.	0.038

Table 4.4.5 Thermal Conductivities of Material for Refrigeration and Extreme Low Temperatures

Material	Bulk density, lb/ft³	Temp, °F	k
Corkboard	6.9	100	0.022
		−100	0.018
		−300	0.010
Fiberglas with asphalt coating (board)	11.0	100	0.023
		−100	0.014
		−300	0.007
Glass blocks, expanded cellular glass	8.5	100	0.033
		−100	0.024
		−300	0.016
Mineral wool board, Rockcork	14.3	100	0.024
		−100	0.017
		−300	0.008
Silica aerogel, powder, Santocel	5.3	100	0.013
		0	0.012
		−100	0.010
Vegetable fiberboard, asphalt coating	14.4	100	0.028
		−100	0.021
		−300	0.013
Foams:			
Polystyrene*	2.9	−100	0.015
Polyurethane†	5.0	−100	0.019

* Test space pressure, 1.0 atm; $k = 0.0047$ at 10^{-5} mmHg.
† Test space pressure, 1.0 atm; $k = 0.007$ at 10^{-3} mmHg.

For L/D less than 60, multiply the right-hand side of Eqs. (4.4.6a), (4.4.6b), and (4.4.6c) by $1 + (D/L)^{0.7}$.

Turbulent Flow of Gases inside Clean Tubes, $DG/\mu_f > 7{,}000$

$$h_m = 0.024 C_p G^{0.8}/(D_i')^{0.2} \tag{4.4.6b}$$

Turbulent Flow of Water inside Clean Tubes, $DG/\mu_f > 7{,}000$

$$h_m = 160(1 + 0.012 t_f) V_s^{0.8}/(D_i')^{0.2} \tag{4.4.6c}$$

Turbulent Flow of Liquid Metals inside Clean Tubes, $C_p\mu/k < 0.05$ The equation of Sleicher and Tribus ("Recent Advances in Heat Transfer," p. 281, McGraw-Hill, 1961) is recommended for isothermal tube walls:

$$\frac{h_m D}{k} = 6.3 + 0.016 \left(\frac{DGC_p}{k}\right)^{0.91} \left(\frac{C_p\mu}{k}\right)^{0.3} \tag{4.4.6d}$$

Turbulent Flow of Gases or Water in Annuli Use Eq. (4.4.6b) or (4.4.6c), with D' taken as the clearance, inches. If the clearance is comparable to the diameter of the inner tube, see Kays and Crawford.

Water in Coiled Pipes Multiply h_m for the staight pipe by the term $(1 + 3.5 D_i/D_c)$, where D_i is the inside diameter of the pipe and D_c is that of the coil.

Turbulent Boundary Layer on a Flat Plate, $V_\infty \rho_f x/\mu_f > 4 \times 10^5$ no pressure gradient

$$\frac{h}{\rho_f C_p V_\infty}\left(\frac{C_p\mu}{k}\right)^{2/3} = \frac{0.0148}{(\rho_f V_\infty x/\mu_f)^{0.2}} \tag{4.4.6e}$$

$$\frac{h_m}{\rho_f C_p V_\infty}\left(\frac{C_p\mu}{k}\right)_f^{2/3} = \frac{0.0185}{(\rho_f V_\infty L/\mu_f)^{0.2}} \tag{4.4.6f}$$

Fluid Flow Normal to a Single Tube, $D_o G/\mu_f$ from 1,000 to 50,000

$$\frac{h_m D_o}{k_f} = 0.26 \left(\frac{D_o G}{\mu_f}\right)^{0.6} \left(\frac{C_p\mu}{k}\right)_f^{0.3} \tag{4.4.7}$$

Gas Flow Normal to a Single Tube, $D_o G/u_f$ from 1,000 to 50,000

$$h_m = 0.30 C_p G^{0.6}/(D_o')^{0.4} \tag{4.4.7a}$$

Fluid Flow Normal to a Bank of Staggered Tubes, $D_o G_{max}/\mu_f$ from 2,000 to 40,000

$$\frac{h_m D_o}{k_f} = K \left(\frac{C_p\mu}{k}\right)_f^{1/3} \left(\frac{D_o G_{max}}{\mu_f}\right)^{0.6} \tag{4.4.8}$$

Values of K are given in Table 4.4.8.

Water Flow Normal to a Bank of Staggered Tubes, $D_o G_{max}/\mu_f$ from 2,000 to 40,000

$$h_m = 370(1 + 0.0067 t_f) V_{sm}^{0.6}/(D_o')^{0.4} \tag{4.4.8a}$$

Table 4.4.6 Thermal Conductivities of Insulating Materials for High Temperatures

Material	Bulk density, lb/ft³	Max temp, °F	k 100°F	300°F	500°F	1,000°F	1,500°F	2,000°F
Asbestos paper, laminated	22.	400	0.038	0.042				
Asbestos paper, corrugated	16.	300	0.031	0.042				
Diatomaceous earth, silica, powder	18.7	1,500	0.037	0.045	0.053	0.074		
Diatomaceous earth, asbestos and bonding material	18.	1,600	0.045	0.049	0.053	0.065		
Fiberglas block, PF612	2.5	500	0.023	0.039				
Fiberglas block, PF614	4.25	500	0.021	0.033				
Fiberglas block, PF617	9.	500	0.020	0.033				
Fiberglas, metal mesh blanket, #900	.....	1,000	0.020	0.030	0.040			
Cellular glass blocks, ave. value	8.5	900	0.033	0.045	0.062			
Hydrous calcium silicate, "Kaylo"	11.	1,200	0.032	0.038	0.045			
85% magnesia	12.	600	0.029	0.035				
Micro-quartz fiber, blanket	3.	3,000	0.021	0.028	0.042	0.075	0.108	0.142
Potassium titanate, fibers	71.5	.....	.....	0.022	0.024	0.030		
Rock wool, loose	8–12	.....	0.027	0.038	0.049	0.078		
Zirconia grain	113.	3,000	.....	.....	0.108	0.129	0.163	0.217

Table 4.4.3 Thermal Conductivities of Miscellaneous Solid Substances*
Values of k are to be regarded as rough average values for the temperature range indicated

Material	Bulk density, lb/ft³	Temp, °F	k
Asbestos board, compressed asbestos and cement	123.	86.	0.225
Asbestos millboard	60.5	86.	0.070
Asbestos wool	25.	212.	0.058
Ashes, soft wood	12.5	68.	0.018
Ashes, volcanic	51.	300.	0.123
Carbon black	12.	133.	0.012
Cardboard, corrugated	...	...	0.037
Celluloid	87.3	86.	0.12
Cellulose sponge, du Pont	3.4	82.	0.033
Concrete, sand, and gravel	142.	75.	1.05
Concrete, cinder	97.	75.	0.41
Charcoal, powder	11.5	63.	0.029
Cork, granulated	5.4	23.	0.028
Cotton wool	5.0	100.	0.035
Diamond	151.	70.	320.
Earth plus 42% water	108.	0.	0.62
Fiber, red	80.5	68.	0.27
Flotofoam (U.S. Rubber Co.)	1.6	92.	0.017
Glass, pyrex	139	200.	0.59
Glass, soda lime	...	200.	0.59
Graphite, solid	93.5	122.	87.
Gravel	116.	68.	0.22
Gypsum board	51.	99.	0.062
Ice	57.5	...	1.26
Kaolin wool	10.6	800.	0.059
Leather, sole	62.4	...	0.092
Mica	122.	...	0.25
Pearlite, Arizona, spherical shell of siliceous material	9.1	112.	0.035
Polystyrene, expanded "Styrofoam"	1.7	...	0.021
Pumice, powdered	49.	300.	0.11
Quartz, crystal, perpendicular to C axis	...	−300.	12.5
		0.	4.3
		300.	2.3
Quartz, crystal, parallel to C axis	...	−300.	25.0
		0.	8.3
		300.	4.2
Rubber, hard	74.3	100.	0.092
Rubber, soft, vulcanized	68.6	86.	0.08
Sand, dry	94.8	68.	0.188
Sawdust, dry	13.4	68.	0.042
Silica, fused	...	200.	0.83
Silica gel, powder	32.5	131.	0.049
Soil, dry	...	68.	0.075
Soil, dry, including stones	127.	68.	0.30
Snow	7–31	32.	0.34–1.3
Titanium oxide, finely ground	52.	1000.	0.041
Wool, pure	5.6	86.	0.021
Zirconia grain	113.	600.	0.11
Woods, oven dry, across grain†:			
Aspen	26.	85.	0.069
Bald cypress	24.	85.	0.063
Balsa	10.	85.	0.034
Basswood	24.	85.	0.058
Douglas Fir	29.	85.	0.063
Elm, rock	48.	85.	0.097
Fir, white	26.	85.	0.069
Hemlock	29.	85.	0.066
Larch, western	36.	85.	0.078
Maple, sugar	43.	85.	0.094
Oak, red	42.	85.	0.099
Pine, southern yellow	35.	85.	0.078
Pine, white	25.	85.	0.060
Red cedar, western	21.	85.	0.053
Redwood	25.	85.	0.062
Spruce	21.	85.	0.052

* The thermal conductivity of different materials varies greatly. For metals and alloys k is high, while for certain insulating materials, such as glass wool, cork, and kapok, it is very low. In general, k varies with the temperature, but in the case of metals, the variation is relatively small. With most other substances, k increases with rising temperatures, but in the case of many crystalline materials, the reverse is true.

† With heat flow parallel to the grain, k may be 2 to 3 times that with heat flow perpendicular to the grain, the values for wool are taken chiefly from J. D. MacLean, *Trans. ASHRAE*, 47, 1941, p. 323.

If one of the temperatures remains constant, as in a condenser or in an evaporative cooler, Eq. (4.4.5a) applies for parallel flow, counterflow, reversed current, and cross flow.

If U varies considerably with temperature, the apparatus should be considered to be divided into stages, in each of which the variation of U with temperature or temperature difference is linear. Then for parallel or counterflow operation, the following relation may be applied to each stage:

$$q = \frac{A[U_2(\Delta t)_{01} - U_1(\Delta t)_{02}]}{\ln [U_2(\Delta t)_{01}/U_1(\Delta t)_{02}]} \qquad (4.4.5b)$$

FILM COEFFICIENTS

The important physical properties which affect film coefficients (see Sec. 3.1) are thermal conductivity, viscosity, density, and specific heat. Factors within the control of the designer include fluid velocity and size and arrangement of the heating surface. With forced flow of gases under the conditions usually met in practice, the flow is turbulent (see Sec. 3) and under these conditions the film coefficient can be greatly increased by increasing the velocity of the fluid at the expense of a greater power requirement. For a given velocity and fluid, the film coefficient depends upon the direction of flow of fluid relative to the heating surface. With free or natural convection, for a given arrangement of surface, the film coefficient depends on an additional fluid property, the coefficient of thermal expansion, on the temperature difference between surface and fluid, and on the local gravitational acceleration. With forced convection at low rates of flow, particularly with viscous fluids such as oils, laminar motion may prevail and the film coefficient depends on thermal conductivity, specific heat, mass rate of flow per tube, and length and diameter of the tube. In any event, the film coefficients h are correlated in terms of dimensionless groups of the controlling factors.

Turbulent Flow inside Clean Tubes (No Change in Phase), $DG/\mu_f > 7{,}000$

$$\frac{h_m}{C_p G}\left(\frac{C_p \mu_f}{k_f}\right)^{2/3} = \frac{0.023}{(DG/\mu_f)^{0.2}} \qquad (4.4.6a)$$

Table 4.4.3 Thermal Conductivities of Miscellaneous Solid Substances*

Values of k are to be regarded as rough average values for the temperature range indicated

Material	Bulk density, lb/ft³	Temp, °F	k
Asbestos board, compressed asbestos and cement	123.	86.	0.225
Asbestos millboard	60.5	86.	0.070
Asbestos wool	25.	212.	0.058
Ashes, soft wood	12.5	68.	0.018
Ashes, volcanic	51.	300.	0.123
Carbon black	12.	133.	0.012
Cardboard, corrugated	...	...	0.037
Celluloid	87.3	86.	0.12
Cellulose sponge, du Pont	3.4	82.	0.033
Concrete, sand, and gravel	142.	75.	1.05
Concrete, cinder	97.	75.	0.41
Charcoal, powder	11.5	63.	0.029
Cork, granulated	5.4	23.	0.028
Cotton wool	5.0	100.	0.035
Diamond	151.	70.	320.
Earth plus 42% water	108.	0.	0.62
Fiber, red	80.5	68.	0.27
Flotofoam (U.S. Rubber Co.)	1.6	92.	0.017
Glass, pyrex	139	200.	0.59
Glass, soda lime	...	200.	0.59
Graphite, solid	93.5	122.	87.
Gravel	116.	68.	0.22
Gypsum board	51.	99.	0.062
Ice	57.5	...	1.26
Kapok wool	10.6	800.	0.059
Leather, sole	62.4	...	0.092
Mica	122.	...	0.25
Pearlite, Arizona, spherical shell of siliceous material	9.1	112.	0.035
Polystyrene, expanded "Styrofoam"	1.7	...	0.021
Pumice, powdered	49.	300.	0.11
Quartz, crystal, perpendicular to C axis	...	−300.	12.5
		0.	4.3
		300.	2.3
Quartz, crystal, parallel to C axis	...	−300.	25.0
		0.	8.3
		300.	4.2
Rubber, hard	74.3	100.	0.092
Rubber, soft, vulcanized	68.6	86.	0.08
Sand, dry	94.8	68.	0.188
Sawdust, dry	13.4	68.	0.042
Silica, fused	...	200.	0.83
Silica gel, powder	32.5	131.	0.049
Soil, dry	...	68.	0.075
Soil, dry, including stones	127.	68.	0.30
Snow	7–31	32.	0.34–1.3
Titanium oxide, finely ground	52.	1000.	0.041
Wool, pure	5.6	86.	0.021
Zirconia grain	113.	600.	0.11
Woods, oven dry, across grain†:			
Aspen	26.	85.	0.069
Bald cypress	24.	85.	0.063
Balsa	10.	85.	0.034
Basswood	24.	85.	0.058
Douglas Fir	29.	85.	0.063
Elm, rock	48.	85.	0.097
Fir, white	26.	85.	0.069
Hemlock	29.	85.	0.066
Larch, western	36.	85.	0.078
Maple, sugar	43.	85.	0.094
Oak, red	42.	85.	0.099
Pine, southern yellow	35.	85.	0.078
Pine, white	25.	85.	0.060
Red cedar, western	21.	85.	0.053
Redwood	25.	85.	0.062
Spruce	21.	85.	0.052

*The thermal conductivity of different materials varies greatly. For metals and alloys k is high, while for certain insulating materials, such as glass wool, cork, and kapok, it is very low. In general, k ... with the temperature, but in the case of metals, the variation is relatively small. With most other substances, k increases with rising temperatures, but in the case of many crystalline materials, the ... is true.

†With heat flow parallel to the grain, k may be 2 to 3 times that with heat flow perpendicular to the grain, the values for wool are taken chiefly from J. D. MacLean, *Trans. ASHRAE*, **47**, 1941, ...

... one of the temperatures remains constant, as in a condenser or in an ...orative cooler, Eq. (4.4.5a) applies for parallel flow, counterflow, ...ed current, and cross flow.

... U varies considerably with temperature, the apparatus should be ...dered to be divided into stages, in each of which the variation of U ... temperature or temperature difference is linear. Then for parallel or ...terflow operation, the following relation may be applied to each ...

$$q = \frac{A[U_2(\Delta t)_{01} - U_1(\Delta t)_{02}]}{\ln [U_2(\Delta t)_{01}/U_1(\Delta t)_{02}]} \tag{4.4.5b}$$

... COEFFICIENTS

...portant physical properties which affect film coefficients (see ...) are thermal conductivity, viscosity, density, and specific heat. ...within the control of the designer include fluid velocity and ...d arrangement of the heating surface. With forced flow of gases ...under the conditions usually met in practice, the flow is turbulent (see Sec. 3) and under these conditions the film coefficient can be greatly increased by increasing the velocity of the fluid at the expense of a greater power requirement. For a given velocity and fluid, the film coefficient depends upon the direction of flow of fluid relative to the heating surface. With free or natural convection, for a given arrangement of surface, the film coefficient depends on an additional fluid property, the coefficient of thermal expansion, on the temperature difference between surface and fluid, and on the local gravitational acceleration. With forced convection at low rates of flow, particularly with viscous fluids such as oils, laminar motion may prevail and the film coefficient depends on thermal conductivity, specific heat, mass rate of flow per tube, and length and diameter of the tube. In any event, the film coefficients h are correlated in terms of dimensionless groups of the controlling factors.

Turbulent Flow inside Clean Tubes (No Change in Phase), $DG/\mu_f > 7{,}000$

$$\frac{h_m}{C_p G}\left(\frac{C_p \mu_f}{k_f}\right)^{2/3} = \frac{0.023}{(DG/\mu_f)^{0.2}} \tag{4.4.6a}$$